

**SYNTHESIS AND CHARACTERIZATION OF NEW  
DITHIENOSILOLE BASED CHROMIC POLYMERS**

**A THESIS SUBMITTED TO  
GRADUATE SCHOOL OF NATURAL AND APPLIED  
SCIENCES  
OF  
ATILIM UNIVERSITY**

**BY  
MOHAMMED AL-JUMAILI**

**IN PARTIAL FULFILMENT OF THE REQUIREMENTS FOR  
THE DEGREE OF MASTER OF SCIENCE**

**IN  
APPLIED CHEMISTRY**

**AT  
THE DEPARMENT OF CHEMICAL ENGINEERING AND  
APPLIED CHEMISTRY**

**APRIL 2015**

Approval of the Graduate School of Natural and Applied Sciences, Atilim University

\_\_\_\_\_  
Prof. Dr. Ibrahim K. Akman

I certify that this thesis satisfies all the requirements as a thesis for the degree of Master of Science.

\_\_\_\_\_  
Prof. Dr. Atilla CİHANER

Head of Department

This is to certify that we have read the thesis “Synthesis and Characterization of New Dithienosilole Based Chromic Polymers” submitted by “MOHAMMED AL-JUMAILI” and that in our opinion it is fully adequate, in scope and quality, as a thesis for the degree of Master of Science.

\_\_\_\_\_  
Prof. Dr. Atilla CİHANER

Supervisor

Examining Committee Members

Prof. Dr. Atilla Cihaner

Assoc. Prof. Dr. Ali Çırpan

Assist. Prof. Dr. Murat Kaya

\_\_\_\_\_  
\_\_\_\_\_  
\_\_\_\_\_  
Date: 21.04.2015

I declare and guarantee that all data, knowledge and information in this document has been obtained, processed and presented in accordance with academic rules and ethical conduct. Based on these rules and conduct, I have fully cited and referenced all material and results that are not original to this work.

Name, Last name: MOHAMMED, AL-JUMAILI

Signature:

## ABSTRACT

# SYNTHESIS AND CHARACTERIZATION OF NEW DITHIENOSILOLE BASED CHROMIC POLYMERS

Al-Jumaili, Mohammed

M.S., Chemical Engineering and Applied Chemistry

Supervisor: Prof. Dr. Atilla Cihaner

April 2015, 51 pages

2-Ethylhexyl substituted dithienosilole based soluble polymers including thiophene (**P1**) and bithiophene (**P2**) units were synthesized via Stille Coupling reaction. The polymers were characterized by using nuclear magnetic resonance (NMR), gel permeation chromatography (GPC), scanning electron microscopy (SEM) and thermal gravimetric analysis (TGA) techniques. The presence of 2-ethylhexyl substituents on the silole ring gave solubility property to the polymers in common solvents. According to GPC measurements, weight average molecular weights of the polymers **P1** and **P2** were found to be as 70977 with a polydispersity index (PDI) of 2.30 and 110439 with a PDI of 1.42, respectively. Fluorescent polymers in toluene solution have maximum emission bands at 634 nm for **P1** and 613 for **P2**. Chemical and electrochemical doping of the polymers in solution and film forms were monitored by using ultraviolet-visible (Uv-vis) spectroscopic technique. The polymers exhibited chromic (chemochromic and electrochromic) properties. While the colors of the neutral polymer films are purple for **P1** and reddish brown for **P2**, both polymers are transparent sky blue at their oxidized states. The band gaps of polymers in film forms were calculated as 1.81 eV for **P1** and 1.92 eV for **P2**. Also, electrochromic device applications of the polymers were done. Electrochemical and optical behaviors of the polymer demonstrated that they can be good candidates for optoelectronic applications.

*Keywords:* Chemical Polymerization, Stille Coupling, Chromism, Dithienosilole, Thiophene.

## ÖZ

# YENİ DİTİYENOSİLOL ESASLI KROMİK POLİMERLERİN SENTEZİ VE KARAKTERİZASYONU

Al-Jumaili, Mohammed

Yüksek Lisans, Kimya Mühendisliği ve Uygulamalı Kimya Bölümü

Tez Yöneticisi: Prof. Dr. Atilla Cihaner

Nisan 2015, 51 pages

Stille kenetlenme tepkimesi ile tiyofen (**P1**) ve bitiyofen (**P2**) içeren 2-etilhekzil sübstitüeli ditiyenosilol esaslı çözünür polimerler sentezlenmiştir. Polimerler nükleer magnetik rezonans (NMR), jel geçirgenlik kromatografisi (GPC), taramalı elektron mikroskobu (SEM) ve termal gravimetrik analiz (TGA) teknikleri kullanılarak karakterize edilmiştir. Silol halkası üzerindeki 2-etilhekzil sübstitüentlerinin varlığı polimerlerin yaygın çözücülerde çözünmesini sağlamıştır. GPC ölçümlerine göre, polimerler **P1** ve **P2**'nin ağırlık ortalama moleküler ağırlıkları sırasıyla 2.30 çok dağılımlılık belirtesi (PDI) ile 70977 ve 1.42 PDI ile 110439 bulunmuştur. Tolüen çözeltisi içerisindeki floresans polimerlerin maksimum ışımaya bantları **P1** için 634 nm ve **P2** için 613 nm'dir. Polimerlerin çözelti ve film formlarındaki kimyasal ve elektrokimyasal katkılandırılmaları morötesi-görünür (UV-vis) spektroskopi tekniği ile görüntülenmiştir. Polimerler kromik (kemokromik ve elektrokromik) özellik göstermektedirler. Nötr polimer filmlerinin renkleri **P1** için mor ve **P2** için kızılımsı kahverengi iken her iki polimer yükseltgen hallerinde geçirgen gökyüzü mavisine sahiptirler. Polimerlerin film formunda band aralıkları **P1** için 1.81 eV ve **P2** için 1.92 eV olarak hesaplanmıştır. Ayrıca, polimerlerin elektrokromik cihaz uygulamaları yapılmıştır. Polimerlerin elektrokimyasal ve optik özellikleri ilgili polimerlerin optoelektronik uygulamalar için iyi birer aday olabileceğini göstermiştir.

*Anahtar Kelimeler:* Kimyasal Polimerizasyon, Stille Kenetlenmesi, Kromizm, Ditiyenosilol, Tiyofen.

**TO MY FAMILY**

## ACNOWLEDGEMENTS

I would like to take this opportunity first and foremost thank God Almighty for being my strength and guide in the writing of this thesis. Without him, I would not have had the wisdom or the physical ability to do so.

I would like to thank my advisor Prof. Dr. Atilla Cihaner for his patient and help and it is a great honor for me to be the first foreign student for him. Thanks for giving me this opportunity to work with him.

To...

Mesopotamia with honour and dignity...

To...

Those, who lost their lives in Iraq without committing any crime...

To...

My father...

My mother...

My wife Sara for her patient and supporting...

My sons Jannat and Moamn...

My brothers and sisters...

For their kindness attention and encouragement...

All my colleagues in Atılım Opto-Electronic Materials and Solar Energy Laboratory (ATOMSEL).

## Table of Contents

<b>ABSTRACT</b> .....	<b>iii</b>
<b>ÖZ</b> .....	<b>iv</b>
<b>DEDICATION</b> .....	<b>v</b>
<b>ACKNOWLEDGEMENTS</b> .....	<b>vi</b>
<b>TABLE OF CONTENTS</b> .....	<b>vii</b>
<b>LIST OF TABLES</b> .....	<b>viii</b>
<b>LIST OF FIGURE</b> .....	<b>ix</b>
<b>LIST OF SCHEMES</b> .....	<b>xi</b>
<b>LIST OF ABBREVIATIONS</b> .....	<b>xii</b>
<b>1. CHAPTER 1: INTRODUCTION</b> .....	<b>1</b>
1.1 Preparation of Conjugated Polymers via Chemical Polymerization Method.....	2
1.2 Preparation of Conjugated Polymers via Electrochemical polymerization.....	3
1.3 Characterization Of Conducting Polymers.....	4
1.4 Conductivity of Conjugated Polymers.....	5
1.5 Band Gap Theory.....	6
1.6 Silole-Based Polymers.....	7
1.6.1 Dithienosilole-Based Polymers.....	7
<b>2. CHAPTER 2: MATERIALS AND METHODS</b> .....	<b>17</b>
2.1 Materials.....	17
2.2 Electroanalytical Studies.....	17
2.3 Opto-electronic Studies.....	17
2.4 Other Characterization Techniques.....	18
2.5 Synthesis of Polymers P1 and P2.....	18
2.6 Construction of Electrochromic Device.....	19
<b>3. CHAPTER 3: RESULTS AND DISCUSSION</b> .....	<b>21</b>
3.1 Characterization.....	21
3.2 Opto-Chemical Properties of the Polymers.....	26
3.3 Opto-Electrochemical Studies.....	35
3.4 Thermal Properties.....	38
3.5 Electrochromic Devices.....	39
<b>4. CHAPTER 4: CONCLUSION</b> .....	<b>41</b>
<b>REFERENCES</b> .....	<b>42</b>

## LIST OF TABLES

<b>Table 1.1</b> Techniques used for characterization of conducting polymers .....	4
<b>Table 3.1</b> Some properties of polymers P1, P2 and their derivatives .....	23
<b>Table 3.2</b> Color changes of P1 dissolved in CH <sub>2</sub> Cl <sub>2</sub> solution after the addition of SbCl <sub>5</sub> .....	27
<b>Table 3.3</b> Color changes of chemically oxidized P1 dissolved in CH <sub>2</sub> Cl <sub>2</sub> solution after the addition of NH <sub>3</sub> .....	28
<b>Table 3.4</b> Color changes of P2 dissolved in CH <sub>2</sub> Cl <sub>2</sub> solution after the addition of SbCl <sub>5</sub> .....	29
<b>Table 3.5</b> Color changes of chemically oxidized P2 dissolved in CH <sub>2</sub> Cl <sub>2</sub> solution after the addition of NH <sub>3</sub> .....	30

## LIST OF FIGURE

<b>Figure 1.1</b> Some examples of conducting polymers .....	1
<b>Figure 1.2</b> Mechanism of the Stille coupling .....	2
<b>Figure 1.3</b> Electrochemical polymerization of thiophene .....	3
<b>Figure 1.4</b> Doping of polythiophene .....	5
<b>Figure 1.5</b> Band gaps for metals, semiconductors and insulators .....	6
<b>Figure 2.1</b> Construction of an electrochromic device .....	20
<b>Figure 3.1</b> <sup>1</sup> H NMR spectra of (a) polymer P1 and (b) polymer P2 in CDCl <sub>3</sub> .....	21
<b>Figure 3.2</b> SEM images of polymers (a)-(b) P1 and (c)-(d) P2.....	24
<b>Figure 3.3</b> Absorbance and emission spectra of the polymers (a) P1 and (b) P2 in toluene. Inset: Pictures of the polymers in toluene under ambient light (left) and handheld UV lamp (right) at 365 nm .....	25
<b>Figure 3.4</b> Changes in optical absorption spectra of chemically obtained P1 dissolved in CH <sub>2</sub> Cl <sub>2</sub> solution after addition of 2 μL (for each spectrum) of 0.01 M SbCl <sub>5</sub> .....	27
<b>Figure 3.5</b> Changes in optical absorption spectra of chemically oxidized P1 dissolved in CH <sub>2</sub> Cl <sub>2</sub> solution after addition of 2 μL (for each spectrum) of 0.5 M NH <sub>3</sub> .....	28
<b>Figure 3.6</b> Changes in optical absorption spectra of chemically obtained P2 dissolved in CH <sub>2</sub> Cl <sub>2</sub> solution after addition of 2 μL (for each spectrum) of 0.01 M SbCl <sub>5</sub> .....	29
<b>Figure 3.7</b> Changes in optical absorption spectra of chemically oxidized P2 dissolved in CH <sub>2</sub> Cl <sub>2</sub> solution after addition of 2 μL (for each spectrum) of 0.5 M NH <sub>3</sub> .....	30
<b>Figure 3.8</b> The coating of the polymers (a)-(d) P1 and (e)-(h) P2 dissolved in CH <sub>2</sub> Cl <sub>2</sub> on ITO surfaces via spray coating method.....	31
<b>Figure 3.9</b> Changes in optical absorption spectra of coated P1 on ITO in acetonitrile after addition of 2 μL (for each spectrum) of 0.1 M SbCl <sub>5</sub> . Inset: Colors of the film at different oxidation states .....	32
<b>Figure 3.10</b> Changes in optical absorption spectra of chemically oxidized P1 on ITO in acetonitrile solution after addition of 2 μL (for each spectrum) of 0.5 M NH <sub>3</sub> . Inset: Colors of the film at different oxidation states .....	32
<b>Figure 3.11</b> Changes in optical absorption spectra of coated P2 on ITO in acetonitrile after addition of 2 μL (for each spectrum) of 0.1 M SbCl <sub>5</sub> . Inset: Colors of the film at different oxidation states .....	33
<b>Figure 3.12</b> Changes in optical absorption spectra of chemically oxidized P2 on ITO in acetonitrile solution after addition of 2 μL (for each spectrum) of 0.5 M NH <sub>3</sub> . Inset: Colors of the film at different oxidation states .....	34

<b>Figure 3.13</b> (a) Scan rate dependence of the polymer film P1 coated on Pt electrode in 0.1 M TBAH/acetonitrile solution at different scan rates (mV/s), a: 40, b: 60, c: 80, d: 100, e: 120, f: 140, g: 160, h: 180 and i: 200. (b) Relationship of anodic and cathodic current peaks as a function of scan rate in 0.1 M TBAH/acetonitrile solution .....	35
<b>Figure 3.14</b> (a) Scan rate dependence of the polymer film P2 coated on Pt electrode in 0.1 M TBAH/acetonitrile solution at different scan rates (mV/s), a: 40, b: 60, c: 80, d: 100, e: 120, f: 140, g: 160, h: 180 and i: 200. (b) Relationship of anodic and cathodic current peaks as a function of scan rate in 0.1 M TBAH/acetonitrile solution .....	35
<b>Figure 3.15</b> Optical absorption spectra of P1 film on ITO in 0.1M TBAH/acetonitrile at various applied potentials upon moving from 0.0 V to 1.5 V.....	36
<b>Figure 3.16</b> Optical absorption spectra of P2 film on ITO in 0.1M TBAH/acetonitrile at various applied potentials upon moving from 0.0 V to 1.5 V .....	37
<b>Figure 3.17</b> TGA thermograms of (a) P1 and (b) P2 .....	38
<b>Figure 3.18</b> Cyclic voltammogram of PEDOT/P1 based electrochromic device at a scan rate of 100 mV/s between -1.8 V and 1.8 V .....	39
<b>Figure 3.19</b> Optical characterization of PEDOT/P1 electrochromic device by applying different potentials between -0.1 V and 1.8 V. The colors of device at -1.0 V and 1.8 V. PEDOT was used as a cathode electrode .....	39
<b>Figure 3.20</b> Cyclic voltammogram of PEDOT/P2 based electrochromic device at a scan rate of 100 mV/s between -1.8 V and 1.8 V .....	40
<b>Figure 3.21</b> Optical characterization of PEDOT/P2 electrochromic device by applying different potentials between -0.1 and 1.8 V. The colors of device at -1.0 V and 1.8 V. PEDOT was used as a cathode electrode .....	40

## LIST OF SCHEMES

<b>Scheme 2.1</b> Synthesis of P1 and P2 via Stille coupling reaction .....	19
---	----

GCPRIS

## LIST OF ABBREVIATIONS

CDCl <sub>3</sub>	-	Deuteriochloroform
DTS	-	Dithienosilole
DCM	-	Dichloromethane
DSC	-	Differential Scanning Calorimetry
E <sub>g</sub>	-	Band Gap Energy
eV	-	Electron-Volt
HOMO	-	Highest Occupied Molecular Orbital
ITO	-	Indium Tin Oxide
LUMO	-	Lowest Unoccupied Molecular Orbital
NMR	-	Nuclear Magnetic Resonance
OFETs	-	Organic Field Effect Transistors
OLEDs	-	Organic Light-Emitting Diodes
PDI	-	Polydispersity Index
PEDOT	-	Poly(3,4-ethylenedioxythiophene)
PCE	-	Power Conversion Efficiency
RE	-	Reference Electrode
SCE	-	Saturated Calomel Electrode
SEM	-	Scanning Electron Microscope
SbCl <sub>5</sub>	-	Antimony Pentachloride
TGA	-	Thermal Gravimetric Analysis
TBAPF <sub>6</sub>	-	Tetrabutylammonium Hexafluorophosphate
TBAH	-	Tetrabutylammonium Hexafluorophosphate
THF	-	Tetrahydrofuran
UV-vis	-	Ultraviolet Visible
WE	-	Working Electrode

# CHAPTER 1

## INTRODUCTION

The conducting (conductive, conjugated) polymers such as polyacetylenes, polyanilines, polypyrroles and polythiophenes (**Figure 1.1**) are studied extensively in industrial and academic areas. Of all the top categories, polyaniline is one of the oldest known conductive polymers. Letheby had been prepared polyaniline firstly in 1862 by the anodic oxidation of aniline in sulfuric acid [1].

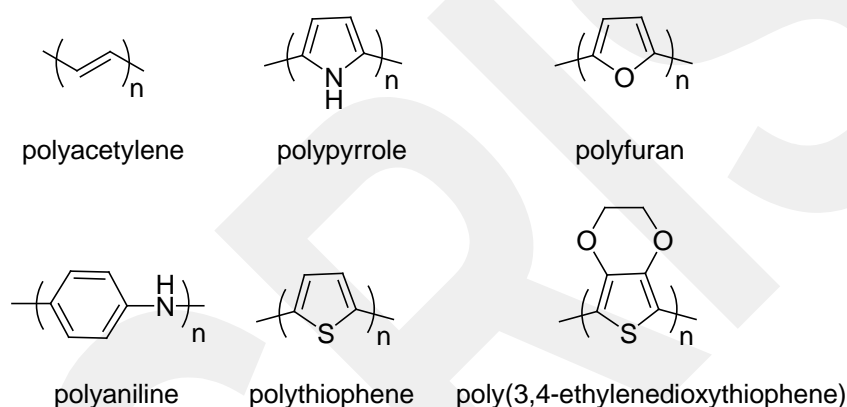


**Figure 1.1** Some examples of conducting polymers.

After the pioneering work of Shirikawa, MacDiarmid and Heeger in 1977 [2], conjugated polymers have attracted the interest of many scientists in academic and industrial areas since they are promising candidates for use in the fields of organic light emitting diodes [3-6], organic photovoltaic devices [7-10], electrochromic displays and devices [11-13], smart windows [14, 15], chemical sensors [16-18], transistors [19, 20] and so forth.

## 1.1 Preparation of Conjugated Polymers via Chemical Polymerization Method

Among all the synthetic methods, chemical polymerization is the most effective and useful technique for the preparation of huge amounts of conjugated polymers. In chemical polymerization method, for example, by the help of chemical oxidant the monomers are oxidized and radical cations are formed. By the coupling of the monomers oligomeric species are formed and during proceeding polymerization long polymer chains are obtained. Conjugated polymers are synthesized by various kinds of cross-coupling reactions such as Suzuki coupling and Stille coupling [21].

The Stille coupling reaction is a very good route to form carbon–carbon bonds which connects  $sp^2$ - $sp^2$  bonds containing molecules [22] (**Figure 1.2**).

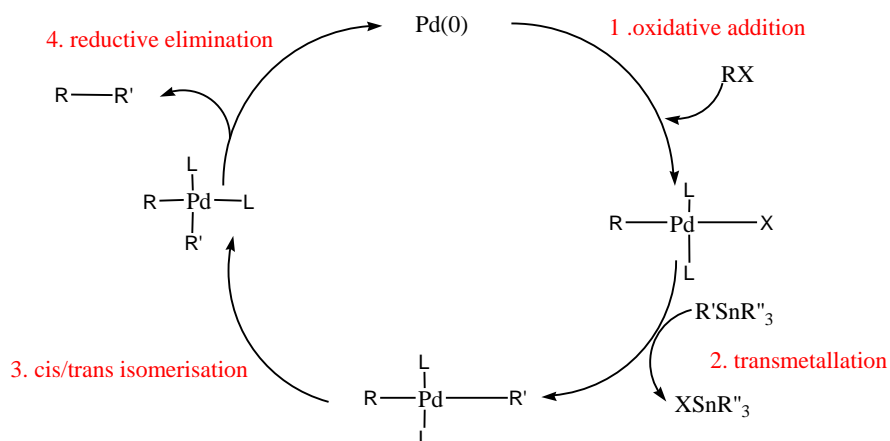


**Figure 1.2** Mechanism of the Stille coupling [23,24].

The Stille coupling has generally high selectivity and broad scope. Its buffering feature towards most functional groups allows the Stille coupling specially effective for transformations of highly functionalized molecules. Thus, it has been successfully applied in the synthesis of a variety of ring systems including delicate functional groups.

## 1.2 Preparation of Conjugated Polymers via Electrochemical Polymerization

### Method

When the electrode substrate is immersed in monomer solution and subjected to electrochemical treatment, the process is called electrochemical polymerization (**Figure 1.3**). The monomers are oxidized or reduced to an activated form which polymerizes on electrode surface. If the polymer is intended to be used as a polymer film electrode, thin layer sensor, in micro technology etc., electrochemical polymerization method is mostly preferred to chemical polymerization since the potential control is critically needed for the production of good-quality material and the polymer film is formed at the desirable spot [25].

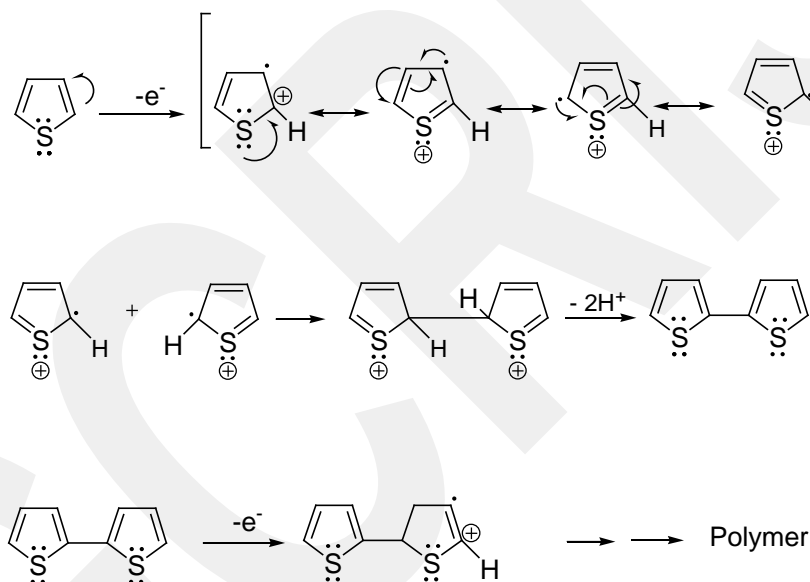


**Figure 1.3** Electrochemical polymerization of thiophene [26].

### 1.3 Characterisation of Conducting Polymers

Electrochemical, chemical and physical characterization of conducting polymers have been carried out by various techniques. **Table 1.1** shows the variety of characterisation techniques that can be used.

**Table 1.1** Techniques used for the characterisation of conducting polymers.

Type	Characterisation Techniques	Information Obtained
Electrochemical Methods	Cyclic Voltammetry Pulse Voltammetry Chronoamperometry Chronopotentiometry	Polymerisation Mechanism Electrochemical Properties
Chemical Composition and Structure	Nuclear Magnetic Resonance (NMR) Raman Spectroscopy Spectroelectrochemistry UV-VIS Spectroscopy	Polymer Composition Electronic Structure Counterion Effect
Physical Properties	Scanning Electronic Microscopy (SEM) Atomic Force Microscopy (AFM) Thermogravimetric Analysis (TGA)	Morphology and Porous Structure Mechanical Properties and Thermal Studies

## 1.4 Conductivity in Conjugated Polymers

To understand the electrical properties of the materials and how electrical conductivity takes place, it is necessary to know more about the doping and band gap theory. Electricity is the movement of charged particles called charge carriers (polarons and bipolarons) that are target to the effect of different potential (**Figure 1.4**). These particles are the electrons and holes of the matter in the solid state or its ions in the liquid and gas states, As electricity is transferring in solid matters by the movement of electrons, it is hopeful that the electrical properties of matters basically depend on the electronic configuration of the matter [27].

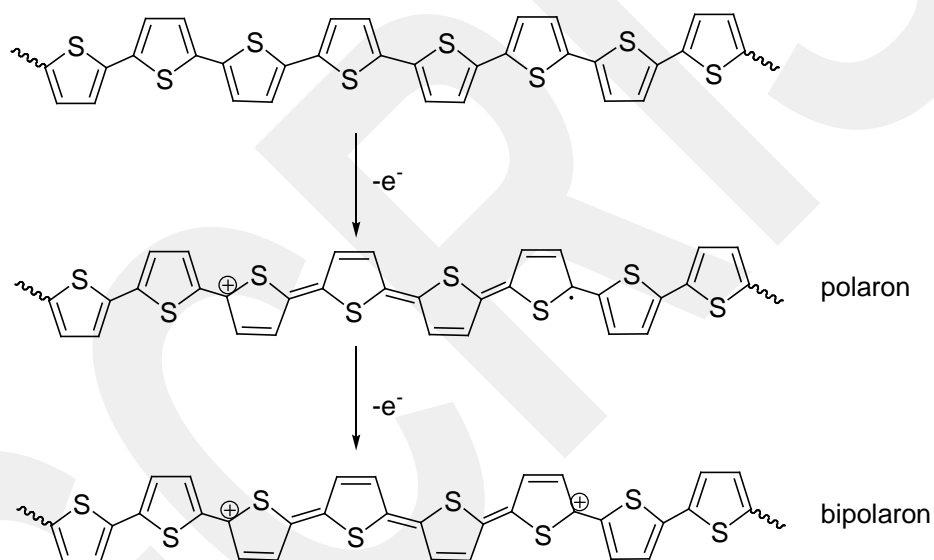


**Figure 1.4** Doping of polythiophene [28].

## 1.5 Band Gap Theory

Band gap can be defined as the energy required to transport electrons from valence band to conductive band. Metals have zero band gap which makes them conductive, while insulators (such as polyethylene) have large band gaps, that means a lot of energy needed for pushing an electron into the conductive band (**Figure 1.5**). On the other hand, semiconductors are between 0.1 and 3 eV, they have small band gaps which make electron transfer possible from valence band to conductive band by applying a little potential energy [29].

Control and adjustment of the band gap in conjugated polymers involve at least six parameters: the length of the bond, alternation of monomer, aromaticity, length of  $\pi$ - coupling conjugation, inter molecular interaction and inter-chain transfer [30].

The highest occupied molecular orbital (HOMO) is filled with the  $\pi$ -electrons in the conjugated polymers and this  $\pi$  system can undergo all kinds of optical and electronic transitions and interactions.

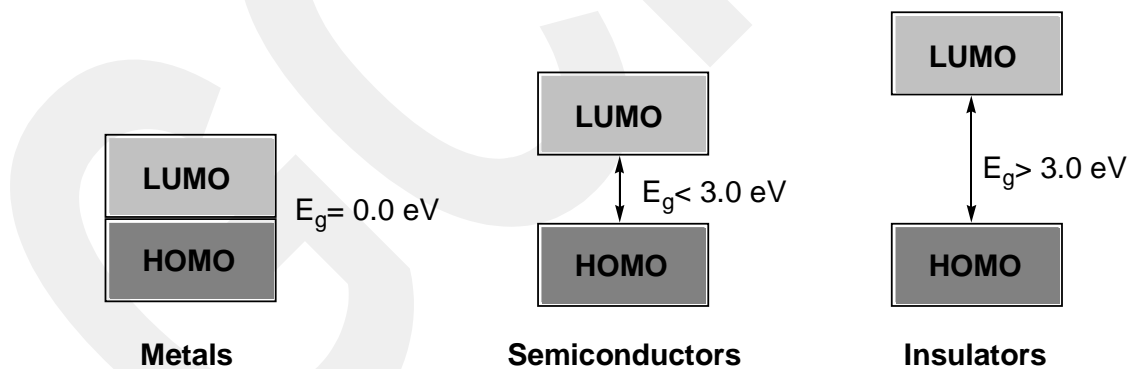


**Figure 1.5** Band gaps for metals, semiconductors and insulators, where HOMO is the highest occupied molecular orbital and LUMO is the lowest unoccupied molecular orbital [31].

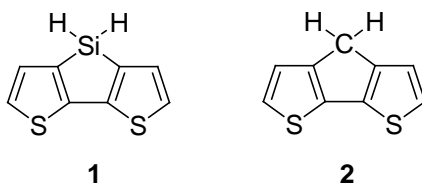
## 1.6 Silole-Based Polymers

Among the members of the conjugated polymers, silole-containing conjugated polymers have been started to expand considerably since silole ring has strong electron affinity, small band gap [32-36] and chemical stability [37]. If these properties are transferred to the corresponding polymer chain, a new door would be opened up to a new member of conjugated polymers.

Experimental and theoretical studies showed that silole ring containing conjugated polymers have low-lying LUMO levels due to their  $\sigma^*-\pi^*$  conjugation characteristic of the silole ring [38-43]. Also, the LUMO level of the silole ring is lower than those of other heterocyclopentadienes, such as furan, pyrrole and thiophene [44,45]. Low LUMO value can result in the small band gap and high electron affinity, which are desired properties in conjugated compounds for being useful in some industrial applications such as electrochromic and electroluminescent devices [46-56], organic field effect transistors (OFETs) [57-69] and organic solar cells [70-83].

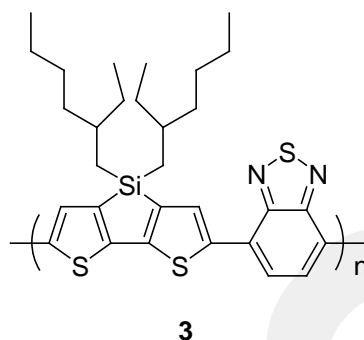
### 1.6.1 Dithienosilole-Based polymers

Ohshita et al. reported a detailed study about silicon-bridged dithienosiloles **1** and demonstrated the decreasing in the LUMO levels (1.75eV) in comparison to methylene bridge analogue **2** which is 2.34 eV [84].



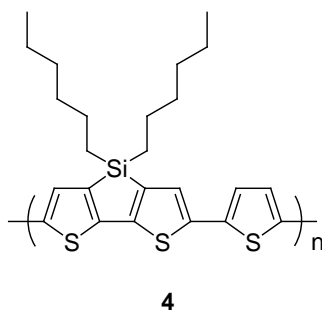
On the other hand, Yang et al. published a study about the synthesis and application of the copolymers **3** including dithienosilole moiety. In this study, 2-ethylhexyl side chains were used to ensure the solubility of the polymer. The polymer **3** was prepared by a Stille coupling reaction. The number average molecular

weight and the PDI of the polymer **3** were found to be as 18 KDa and 1.2, respectively.

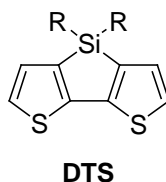


The corresponding polymer has fine properties including reversible n- and p-doping processes. It also has reasonable HOMO and LUMO energy levels, which allows application of photovoltaic cell. The resulting photovoltaic device has a power conversion efficiency (PCE) of 5.1 % and in terms of the response range, all the visible region is covered. Moreover, the hole mobility of the dithienosilole based polymer is  $3 \times 10^{-3} \text{ cm}^2 \text{ V}^{-1}$  which is three times higher than its carbon analogue [85].

On the other hand, Marks and his colleagues investigated the properties of the copolymers **4** bearing thiophene and dithienosilole units with linear hexyl chains on silicon atom. The related processable polymers were synthesized via Stille coupling reactions and the polymers are promising candidate for use in OFETs [86].



Among the photovoltaic donor materials including high efficiency donor-acceptor systems, dithienosilole (DTS) is a well-used donor unit. DTS unit containing conjugated systems exhibit broader absorption in the visible region, relatively lower HOMO energy level and greater hole mobility [87].



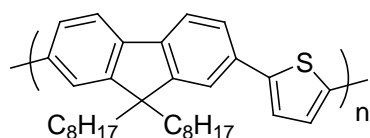
Development of new low-band gap p-type materials and good morphology in donor-acceptor interpenetration systems have been brought a significant accomplishment in this field with PCEs of 7% for solution-processed polymer solar cells [88].

It was seen that the silole-based materials can be synthesized in high yields, which indicated that the polymer with higher molecular weight can stack much better due to the stronger  $\pi$ - $\pi^*$  interaction and was found to offer better charge transfer [89].

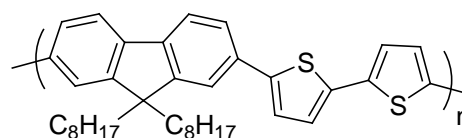
Under the light of this feature, those polymers have been extremely investigated over the past decade industrially as well as in academia. According to the target mentioned above, some novel solution-processed copolymers were reported and compared in the literature.

Two new fluorene-containing copolymers **5** and **6** were synthesized by Suzuki coupling reaction and then fully characterized. They are soluble in hot toluene and chlorobenzene. Copolymer **5** showed higher melting temperature above 400 °C, indicating a good thermal stability. The optical band gaps for copolymers **5** and **6** are calculated to be 2.4 eV and 2.5 eV, respectively. While the molecular weight of the copolymer **5** was measured as 80 Kda with a PDI of 3.3 as well as an absorption band at 456 nm in solution form and at 460 nm in film form, the molecular weight of the copolymer **6** was measured to be 17 KDa with a PDI of 2.6 as well as an absorption band at 427 nm in solution form and at 440 nm in film form. These

copolymers are environmentally stable, and the resulting solution-processed films act as efficient hole transporters in field effect transistor devices.

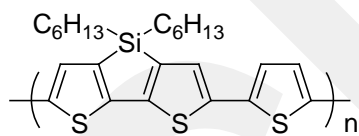


**5**

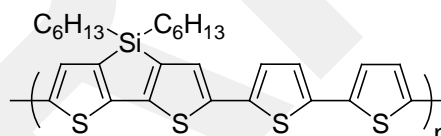


**6**

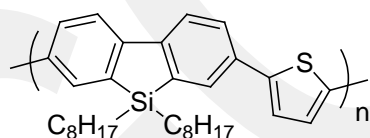
The thienosilole-based homopolymer, as well as its copolymers with mono- and bi-thiophene sub-units (**7** and **8**) were reported by Usta et al. They examined the consequences of introducing thienosilole and benzosilole structures into the thiophene polymer backbone by making comparison of the new benzosilole-based homopolymer and copolymers with mono- and bithiophene sub-units (**9** and **10**) with their carbon analogs (**5** and **6**) [90].



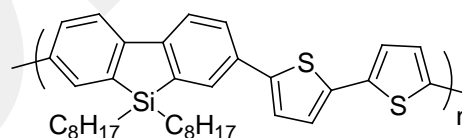
**7**



**8**



**9**



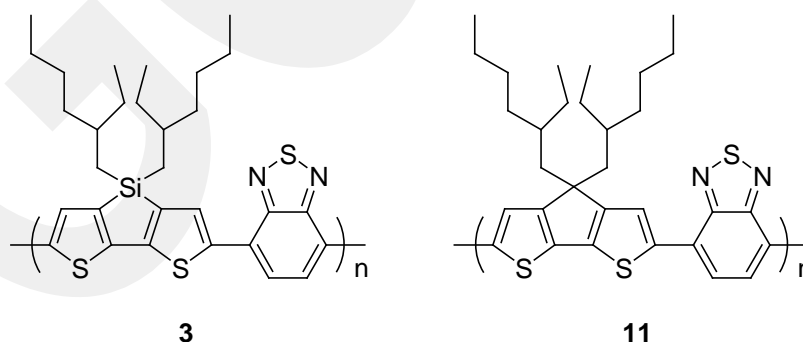
**10**

Thiophene-based copolymers were synthesized by Stille coupling reactions, while phenylene-based copolymers were prepared by Suzuki coupling reactions which was showed that the reaction types are the best suitable ones in them. The PDIs of thiophene-based copolymers (**7** and **8**) were found to be 2.9 and 3.0, respectively, and their molecular weights are measured as 30 KDa for the copolymer **7** and 41 KDa for the copolymer **8**. The absorption maxima values were given as 521 nm for the copolymer **7** and 544 nm for the copolymer **8**. Also, the band gaps were found to be as 2.0 eV for the copolymer **7** and 1.9 eV for the copolymer **8**. On the

other hand, while the PDIs of the copolymers **9** and **10** have the values of 3.1 and 3.7, respectively, they have high molecular weights of 112 KDa for the copolymer **9** and 127 KDa for the copolymer **10**. The maximum absorption wavelengths are 484 nm with a band gap of 2.5 eV for the copolymer **9** and 493 nm with a band gap of 2.3 eV for the copolymer **10**. It can be easily concluded that the copolymers **9** and **10** have higher molecular weights than those of the copolymers **7** and **8**.

When compared to phenylene-based copolymers, charge carrier mobilities were found to be higher in thiophene-based copolymer **8**. Non-encapsulated OFETs were proven to be highly stable in air. This was due to the absence of alkyl side groups on the thiophene ring in contrast to regioregular poly(3-hexylthiophene). All reported silole-containing copolymers have excellent thermal stability. There was no significant weight loss up to 400 °C on TGA analysis. The absorption maxima values of benzosilole-based copolymers were red-shifted by 40-50 nm vs fluorene-based analogues **5** and **6**, confirming Si  $\sigma^*$ -orbital overlaps with the  $\pi$ -conjugated chromophore [91].

Because of its high solubility, the copolymer **3** with branched 2-ethylhexyl silicon substituents was of specific interest for wet processing.. The copolymer is environmentally stable up to 250 °C in air. The optical band gap of the copolymer **3** was determined as 1.45 eV, similar to its carbon analogue polymer **11**.

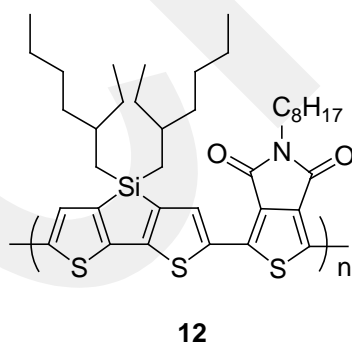


In OFET, the hole mobility for copolymer **3** was found to be  $3 \times 10^{-3} \text{ cm}^2/(\text{V s})$  which is three times higher than its analogues polymer **11**. The copolymer **11** has been proven to be a useful material for organic photovoltaic devices due to its

characteristic behaviour. It also indicated absorption peak around 705 nm in solution form and 730 nm in film form. In addition, the presence of two alkyl side chains resulted in excellent solubility in commonly used solvents, which is important for the formation of uniform films by the spin coating process [92].

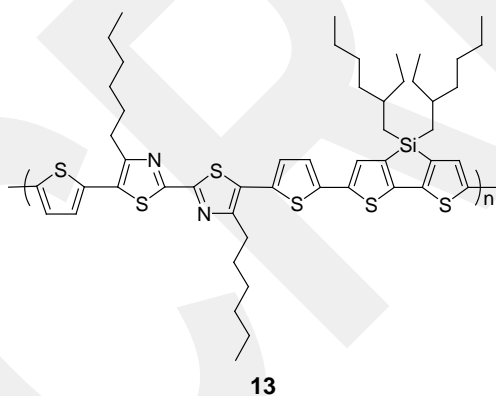
As a result, the polymers with thienosilole and benzosilole building blocks are promising classes of functional materials. Their electronic and optical properties showed the suitability of usage in thermally and environmentally stable organic electronic devices.

Besides, there is a valuable information that a low band gap (1.73 eV) and a deep HOMO energy level (5.57 eV) can be obtained simultaneously from an alternating copolymer **12**. Dithienosilole unit brings some advantages over its carbon-bridged counterpart such as a better hole-transport property and a lower HOMO energy level. The alternating copolymer **12** was prepared by a Stille coupling. The purified polymer has a number-average molecular weight of 28 Kda with a PDI of 1.6 and a band gap of 1.73 eV.

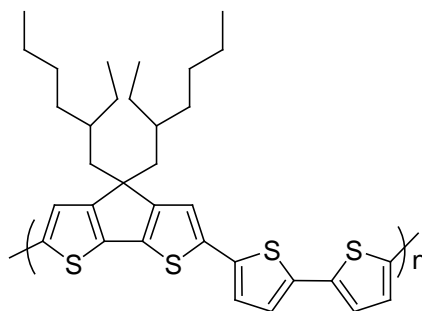


The branched alkyl chains on the dithienosilole unit gave good solubility feature to the polymer, which is a critical parameter for applications in large-scale device production. The copolymer **12** has an excellent solubility in a wide range of organic solvents such as chloroform, chlorobenzene, dichlorobenzene, etc [93].

In order to improve the properties of the synthesized conjugated molecules (e.g., increase the visible absorption and decrease the HOMO energy level), donor-acceptor copolymers of electron-rich (or donor) and electron-deficient (or acceptor) aromatic units were began to be designed and synthesized in recent years. The copolymer **13** containing bithiazole and dithienosilole units in the main chain were the aim of study to find a new conjugated polymer for photovoltaic donor materials by using the Pd-catalyzed Stille-coupling. The resulting polymer showed good solubility in common organic solvents like chloroform, toluene, and chlorobenzene. The molecular weight was determined by GPC analysis as 9.5 KDa with a PDI of 1.7. Its solution form showed an absorption band at 511 nm and the film form gave the maximum absorbance around 558 nm. The band gap was found to be as 1.85 eV. Thiazole unit played an important additive role since it is a well-known electron-deficient unit of containing one electron-withdrawing nitrogen of imine (C=N) [94].

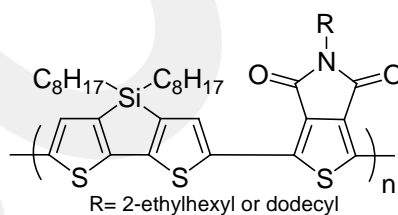


Due to the forced coplanarity of two thienyl sub-units in the chain, the copolymer of bithiophene and cyclopenta [2,1-b:3,4-b']dithiophene were found to be an eminent building block for the conjugated polymers. The copolymer **14** can be easily functionalized by alkyl groups which increased the solubility without causing extra folding of repeating units in the resulting polymer. The copolymer showed a number average molecular weight of 15 KDa with a band gap of 2.35 eV. Its solution form showed a maximum absorption at 548 nm and its film displayed the strongest absorbance band at around 554 nm. It can be concluded that the polymer films generally have longer absorption maxima than the corresponding solutions due to interchain involvement in their solid states [95].



14

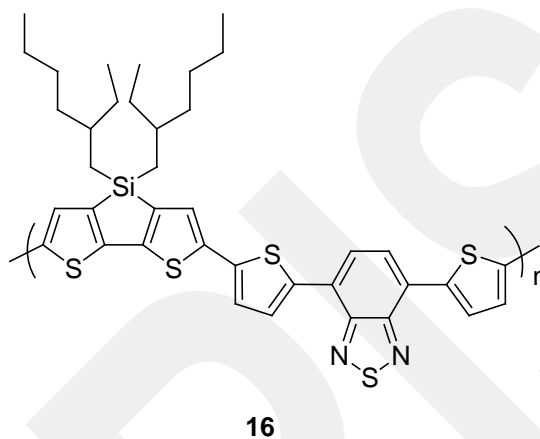
When copolymerized with dithienosilole (DTS) due to its symmetric and coplanar structure with strong electron withdrawing properties, thieno[3, 4-c] pyrrole-4, 6-dione has recently showed promising results as a building block for organic solar cells. Two types of alkyl chains were chosen in order to evaluate the effect of different side chains on copolymer **15**; a branched 2-ethylhexyl and a linear dodecyl group. Both of the copolymers were readily soluble in common organic solvents such as chloroform and tetrahydrofuran. Number average molecular weight and PDI values were found to be as 20 KDa and 2.58 for the polymer bearing ethylhexyl chains and 27 KDa and 2.56 for the polymer bearing dodecyl chains, respectively. The band gaps of both polymers were 1.7 eV. The UV-vis spectrum of the device showed very broad absorption between 400 and 730 nm [96].



15

Silole-containing conjugated polymers with suitable low-lying LUMO levels, low band gaps, and high carrier mobilities have been designed and developed for many years in order to meet the requirements of good polymer photovoltaic materials. The copolymer **16** was synthesized by Stille coupling reaction, and this material was readily dissolved in common solvents. The corresponding weight average molecular weight of the copolymer **16** was 8.0 KDa with a narrow PDI of 1.2. The absorption bands in solution placed at 630 nm and 652 nm for solid thin

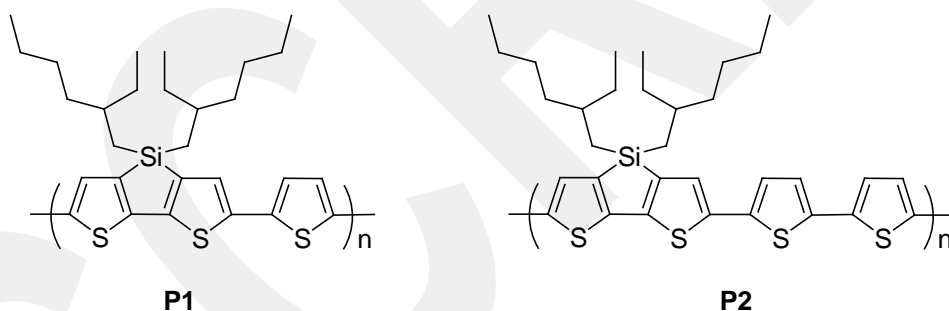
films. The symmetrical ethylhexyl side chains can form  $\pi$ - $\pi^*$  stacking more easily and the polymer **16** has a stronger crystalline tendency due to less steric hindrance in the ethylhexyl side chains. The band gap was calculated as 1.53 eV. It showed that the development of dithienosilole units bearing different side chain lengths could become a promising method for producing highly efficient polymer photovoltaic materials [97].



## 1.7 Aim of the Study

It can be easily concluded that the dithienosiloles have superior properties for optoelectronic applications and by using dithienosilole units efficient materials can be design to tune the energy levels. In this study, 4,4-di-2-ethylhexyl-dithieno[3,2-b:2',3'-d]silole is chosen as the dithienosilole source due to its excellent electron mobility and efficient charge transfer. The alkyl groups are added to improve solubility and complete the overall planar structure [98].

On the other hand, thiophene is the most common basic donor units and the electron density can be more delocalized due to its less aromatic nature which can lower the bond length alternation and increase the conjugation. Herein, under the light of aforementioned properties of dithienosilole based polymers, the synthesis and electro-optical properties of processible conjugated copolymers (**P1** and **P2**) containing alkyl substituted dithienosilole and thiophene units were reported.



The polymers were synthesized via Stille coupling reaction and the obtained polymers were characterized via NMR, UV-vis, floresance, GPC, SEM and electroanalytical techniques. TGA and DSC were used for thermal ansils. After the investigation of the chromic properties of the polymers, electrochromic device applications were performed.

## CHAPTER 2

### MATERIALS AND METHODS

#### 2.1 Materials

All chemicals, except for 2-6-dibromo-(4,4-di-2-ethylhexyl-ithieno(3,2,b:2',3'-d)silole) (Lumtec Company), were purchased from Aldrich Chemical and used as received unless otherwise noted.

#### 2.2 Electroanalytical Studies

0.1 M tetrabutylammonium hexafluorophosphate (TBAH) dissolved in acetonitrile was used as an electrolyte solution for cyclic voltammetric studies. A platinum disk ( $0.0314 \text{ cm}^2$ ) and a platinum wire were used as working and counter electrodes, respectively, as well as a Ag/AgCl reference electrode (calibrated externally using 1 mM solution of ferrocene/ferrocenium couple which is an internal standard calibrated to be 400 mV in acetonitrile solution vs. Ag/AgCl/3M NaCl). The polymer films were formed on Pt disc electrode by dropping the polymer solution on Pt surface and making it dry. Electro-optical properties were investigated by using an indium tin oxide (ITO, Delta Tech. 8–12  $\Omega$ , 0.7 cm  $\times$  5 cm) electrode as well as a platinum wire as a counter electrode and an Ag wire as a pseudo-reference electrode.

#### 2.3 Opto-electronic Studies

For the spectroelectrochemical measurements, the polymer films were coated on ITO substrate via a spray casting technique (Deluxe Professional Airbrush by Aztek A4709). Electroanalytical measurements were performed using a GamryPCI4/300 potentiostat–galvanostat. The redox behaviors of the polymer films were equilibrated by switching between their neutral and oxidized states several times; therefore, the electro-optical results can be obtained repeatedly. The electro-optical spectra were monitored on a Specord S600 spectrometer. Emission measurements were done by Thermo Lumina Florescence Spectrometer. Photographs

of the polymer films were taken by using a Canon (PowerShot A75) digital camera. Colorimetric measurements were recorded on Specord S600 (standard illuminator D65, field of width 10 observer) and color space was given by the international Commission of Illumination with luminance (L), hue (a), and intensity (b). Platinum cobalt DIN ISO 621, iodine DIN EN 1557, and Gardner DIN ISO 6430 are the references of colorimetric measurements.

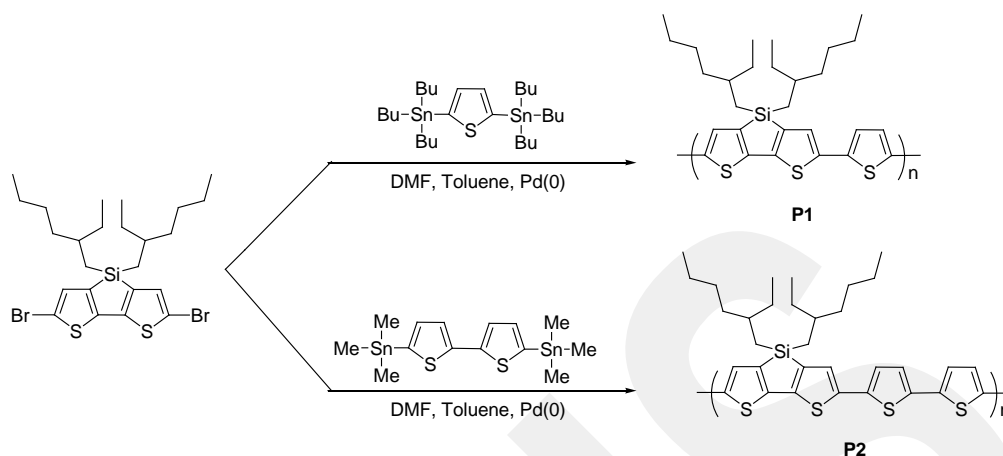
#### 2.4 Other Characterization Techniques

$^1\text{H}$  NMR spectra of obtained polymers were recorded on a Bruker Spectrospin Avance DPX-400 Spectrometer with  $\text{CDCl}_3$  and chemical shifts were given relative to tetramethylsilane as the internal standard. Chemical shifts are reported in terms of ppm and that of  $\text{CDCl}_3$  is 7.26 ppm. Molecular weight measurement was performed via Shimadzu LC-20A/Prominence GPC according to polystyrene standards. Scanning electron microscope (SEM) analysis was monitored by using Quanta 200 FEG Model, Bilkent University Location: UNAM-M03. TGA analysis performed via Q500 Model and DSC device Model 204-F1.

#### 2.5 Synthesis of Polymers P1 and P2

Polymerization was carried via Stille coupling reaction (**Scheme 2.1**). 0.2 mmol of 2,6-dibromo-(4,4-di-2-ethylhexyl-dithieno[3,2-b:2',3'-d]silole) (115 mg) and 0.2 mmol of 2,5-bis(tributylstannyl)thiophene (132 mg) (or 5,5'-bis(trimethylstannyl)2,2'-bithiophene (98 mg)) were placed in a mixture of 2 mL of anhydrous dimethylformamide and 8 mL of toluene and purged with argon gas for 20 min. Then,  $\text{Pd}(\text{PPh}_3)_4$  (10 mg) was added to the reaction flask and the mixture was heated at reflux under argon atmosphere. The reaction was followed by thin layer chromatography. After 16 hours, the reaction mixture was allowed to cool to room temperature, and was poured into methanol (50 mL). The dark brown precipitate was collected via filtration. The precipitate was further purified by a Soxhlet extractor in order of methanol, hexane and finally chloroform to collect the soluble product. The resulting polymer was re-precipitated in methanol and then filtrated and dried under

vacuum. Both polymers **P1** and **P2** were obtained as purple solids in yields of 88.5 % and 67.0%, respectively.



**Scheme 2.1** Synthesis of **P1** and **P2** via Stille coupling reaction.

## 2.6 Construction of Electrochromic Device

An electrochromic material is the one that changes its color by applying a certain potential. This phenomenon is called electrochromism. Electrochromism is the reversible and visible change in transmittance and/or reflectance that is related to an electrochemically induced oxidation–reduction reaction. It results from the appearance of different visible region electronic absorption bands on switching between redox states [99].

On the other hand, an electrochromic device is the system constructed by sandwiching two electrodes (one of two polymer films is in its oxidized state and the other is in its neutral state) and a gel electrolyte between them.

The device was constructed using the electrochromic electrode (**P1** or **P2**) separated by gel electrolyte from a charge balancing counter-electrode poly(3,4-ethylenedioxythiophene) (PEDOT) (**Figure 2.1**). Polymer **P1** film (or **P2** film), dissolved 10 mg sample in 1 mL of chloroform, was coated on ITO by using a spray coating device. Gel electrolyte was prepared using TBAPF<sub>6</sub>:acetonitrile:poly(methyl

methacrylate):propylene carbonate in the ratio of 3:70:7:20 by weight [100]. Square wave potential method was used to investigate the switching ability of the device between various redox states.

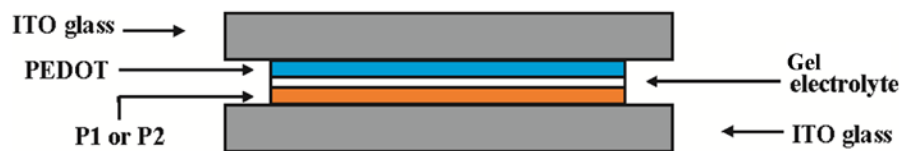


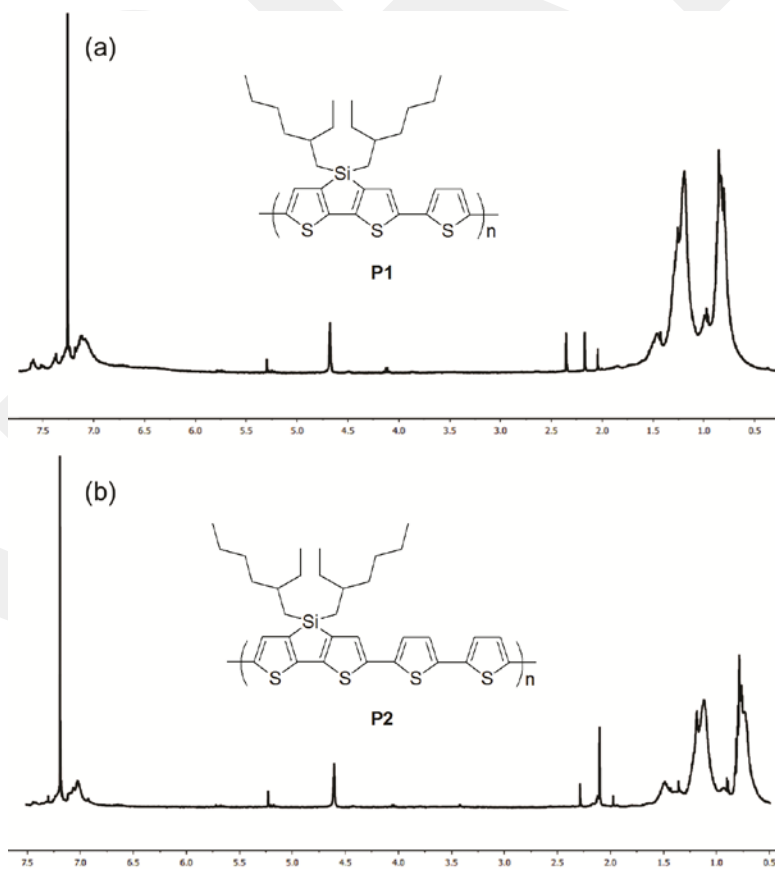
**Figure 2.1** Construction of an electrochromic device.

## CHAPTER 3

### RESULTS AND DISCUSSION

#### 3.1 Characterization

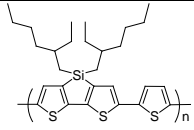
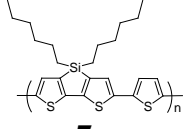
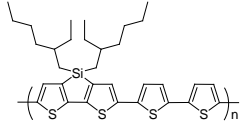
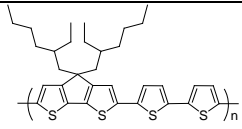
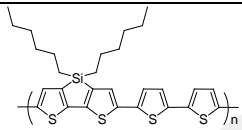
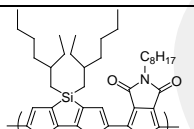
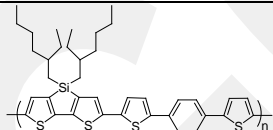
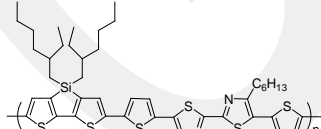
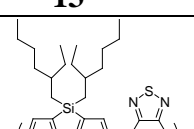
Polymers **P1** and **P2** containing of ethylhexyl substituted dithienosilole and thiophene units were synthesized chemically via Stille coupling reaction. Initial characterization of the polymers was performed by  $^1\text{H}$  NMR analysis (**Figure 3.1**). It can be easily seen that while the presence of ethylhexyl alkyl chain could be confirmed by broad peaks between 0.4 and 1.8 ppm, the broad peaks observed at a wide range from 6.8 to 7.8 ppm could be attributed to the aromatic hydrogens of dithienosilole and thiophene units.



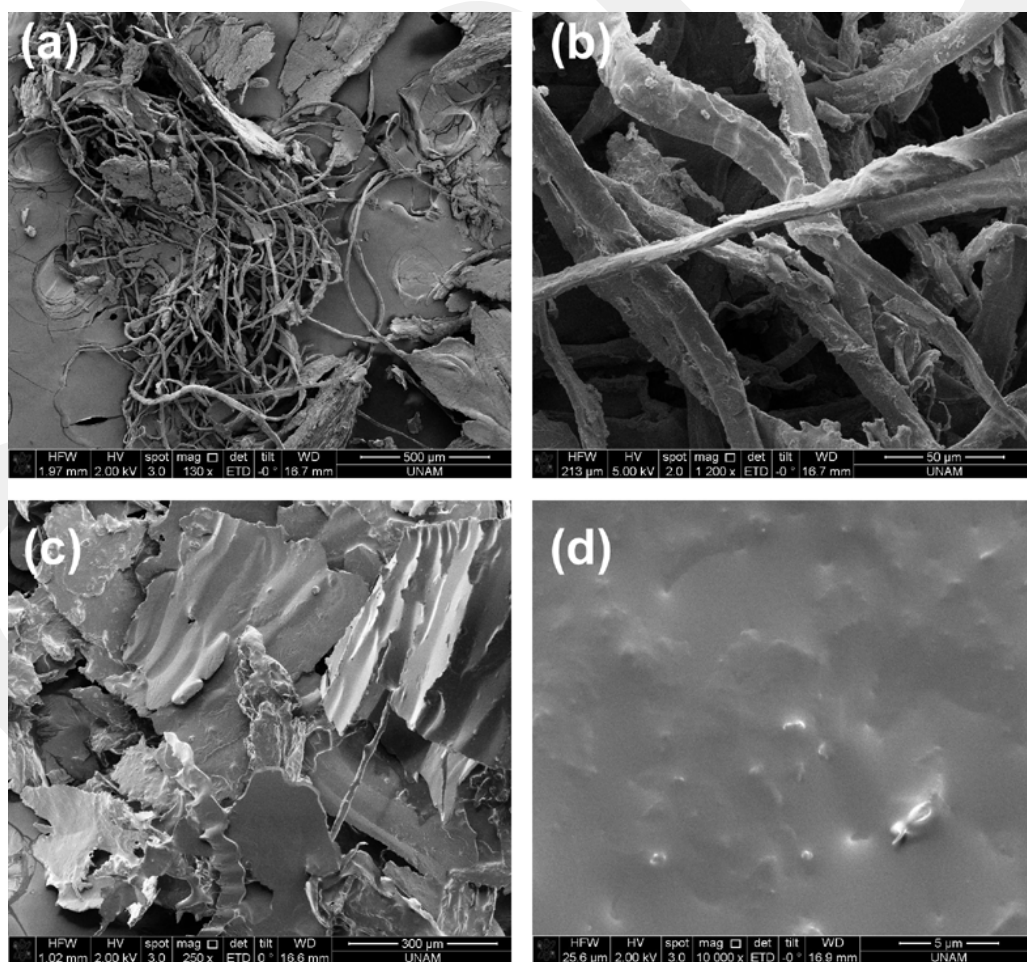
**Figure 3.1**  $^1\text{H}$  NMR spectra of (a) polymer **P1** and (b) polymer **P2** in  $\text{CDCl}_3$ .

On the other hand, the molecular weights of the polymers were determined by GPC analysis using polystyrene as a standart. In chloroform, GPC measurement yielded about 70977 for **P1** with a PDI of 2.30 and 110439 for **P2** with a PDI of 1.42 as the weight average molecular weight. When compared to their linear hexyl analogues [90,91]. The polymers **P1** and **P2** exhibited somewhat narrower molecular weight distribution (see **Table 3.1**). This result can be mainly due to the kind of used polymerization technique (Suzuki coupling) and the purification method of the crude product. For example, the copolymers **7** and **8** were purified only by the precipitation of the products in methanol after polymerization reaction, which coludn't be enough to remove some oligomeric species from the medium.

**Table 3.1** Some properties of polymers **P1**, **P2** and their derivatives.

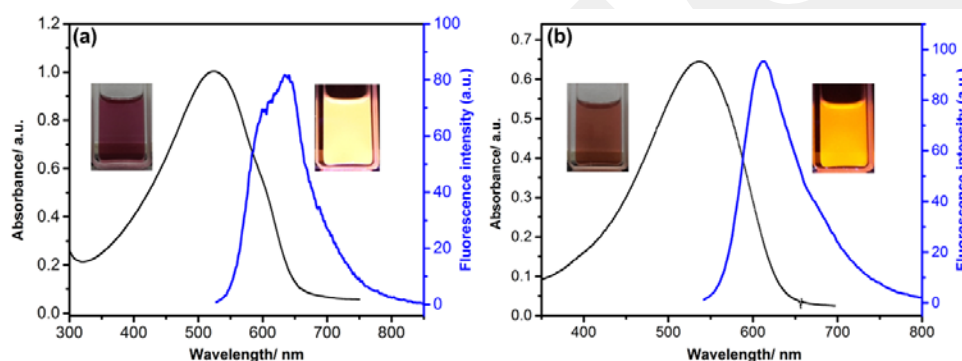
Polymer	$M_w$ (PDI)	$\lambda_{soln}$ (nm) ( $E_g$ (eV))	$\lambda_{film}$ (nm) ( $E_g$ (eV))
 <b>P1</b>	70977 (2.30)	524 (1.90)	539 (1.81)
 <b>7</b> [90]	30000 (2.9)	521 (2.00)	574 (1.80)
 <b>P2</b>	110439 (1.42)	539 (1.96)	537 (1.92)
 <b>14</b> [95]	15000 (1.6)	548 (2.35)	554 (1.4)
 <b>8</b> [91]	41000 (3.0)	544 (1.90)	545 (1.90)
 <b>12</b> [93]	28000 (1.6)	500 (1.83)	717 (1.73)
 <b>16</b> [97]	8000 (1.2)	630 (1.82)	652 (1.53)
 <b>13</b> [94]	9500 (1.7)	511 (2.09)	558 (1.85)
 <b>3</b> [85]	18000 (2.6)	670 (1.78)	740 (1.45)

In electrochemically obtained conducting polymers, a ‘cauliflower’ type morphology has generally been observed and this morphology suggests that the polymer growth process takes place after the formation of a nucleation step. On the other hand, chemically obtained polymers can exhibit various morphology due to the difference in polymerization method when compared to electrochemical polymerization. SEM studies on **P1** and **P2** polymers exhibited two different morphologies shown in **Figure 3.2**. Interestingly, while the polymer **P1** has fibers with a diameter of about 20  $\mu\text{m}$  as well as the formation of sheets layer by layer, polymer **P2** has sheets layer by layer. Though not clear yet, such geometry might probably arise from the fact that the number of used thiophene units in polymerization, which can hinder the formation of fibers.



**Figure 3.2** SEM images of polymers (a)-(b) **P1** and (c)-(d) **P2**.

Solubility is one of the most important problems in the application of the conjugated polymers in industrial areas. For example, the soluble and processable electrochromic polymers have attracted more attention than their insoluble analogues. The corresponding polymers **P1** and **P2** were mostly soluble in common organic solvents such as tetrahydrofuran, chloroform and dichloromethane. **Figure 3.3** showed the absorption spectra and the color of the polymers dissolved in toluene. **P1** has a maximum wavelength at 524 nm with a purple color, whereas **P2** has a maximum wavelength of 539 nm with a reddish brown color. When compared to **P1**, the longer wavelength of **P2** can be attributed to the longer polymer chain.

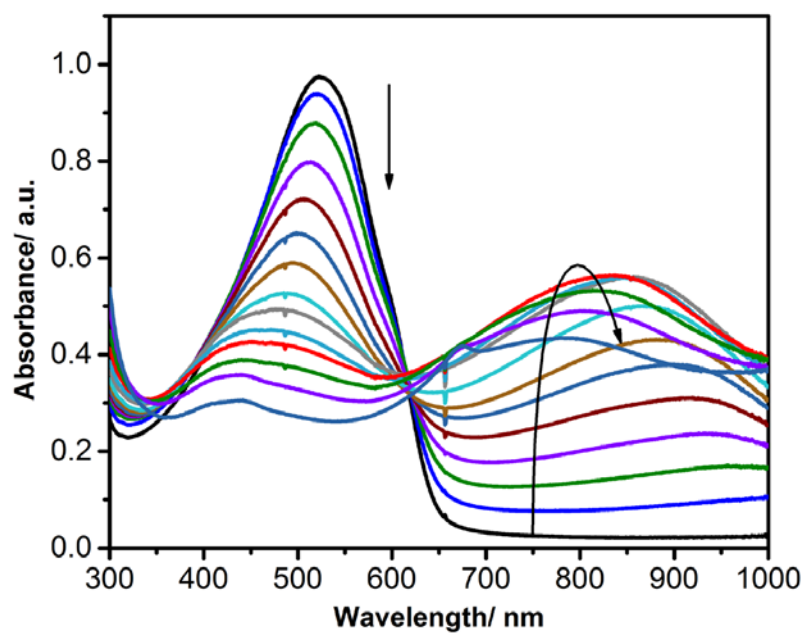


**Figure 3.3** Absorbance and emission spectra of the polymers (a) **P1** and (b) **P2** in toluene. Inset: Pictures of the polymers in toluene under ambient light (left) and handheld UV lamp (right) at 365 nm.

The fluorescence properties of the polymers were also studied in toluene. The polymers **P1** and **P2** showed broad emission bands with maximum wavelengths centered at 634 nm with a shoulder at 598 nm and 613 nm, respectively (**Figure 3.3**). While the polymer **P1** emits yellow color, **P2** emits orange color under UV lamp. At first sight, the observed colors of emission are not appropriate to the emission bands, but it can be conjectured that the observed shoulder at 598 nm for **P1** is dominant to determine the color of emission. On this basis, it can be safely hoped that these soluble polymers can be promising candidates for applications in various fields such as organic lasers and electroluminescent materials. Also, they can be taken into account in light emitting diodes as a yellow/orange light emitter.






### 3.2 Opto-Chemical Properties of the Polymers

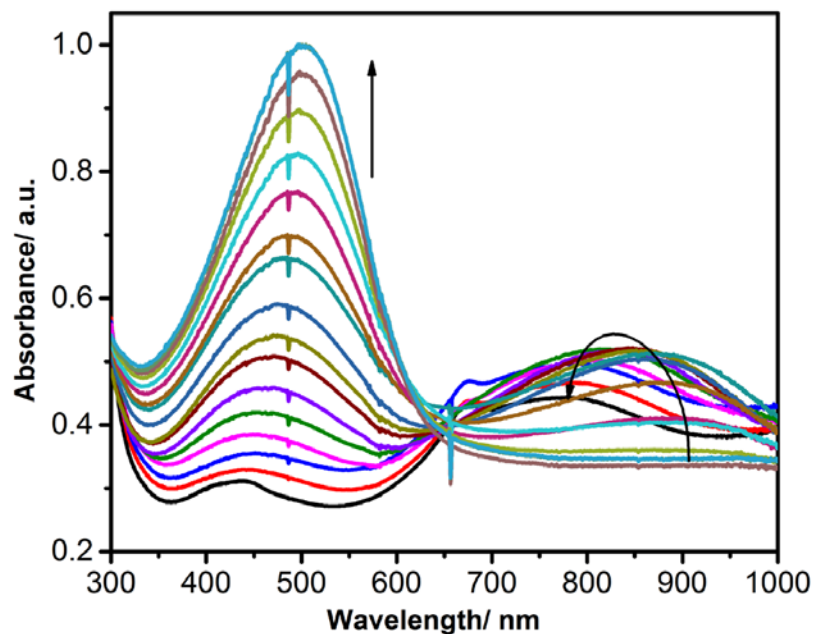
The color of the polymers can be tuned by chemical oxidation. For example, **P1**'s color can be tuned from purple to transmissive green/blue by chemical oxidation. Antimony pentachloride ( $\text{SbCl}_5$ ) is a strong and colorless oxidant. The addition of a very dilute solution of  $\text{SbCl}_5$  dissolved in  $\text{CH}_2\text{Cl}_2$  solution to the polymer solution will change its optical spectrum as well as its color (**Table 3.2**). As shown in **Figure 3.4**, the polymer **P1** solution has a broad absorption band centered at 524 nm attributed to the  $\pi$ - $\pi^*$  transition band. The band gap ( $E_g$ ) of **P1** was determined from the lowest energy end of the  $\pi$ - $\pi^*$  transitions and found as 1.90 eV, which is somewhat smaller than its hexyl analogue (2.0 eV) in solution [90]. By the addition of  $\text{SbCl}_5$ , this transition band started to lose its intensity step by step with a concomitant increase after 700 nm due to the formation of polaron charge carriers. After the addition of a certain amount of  $\text{SbCl}_5$ , the  $\pi$ - $\pi^*$  transition nearly disappeared and shifted to 441 nm. The percent transmittance change ( $\Delta T\%$ ) at 524 nm was calculated as 21%. Upon oxidation, the absorption band of the polaron reached a maximum intensity and then decreased. During this observation, a new charge carrier called bipolaron charges was formed and confirmed by the appearance of a new band beyond 850 nm. The color of the polymer **P1** at neutral state was changed from purple to transmissive red, and to transmissive green/blue during chemical oxidation (**Table 3.2**). On the other hand, by the use of  $\text{NH}_3$ , the polymer couldn't be reduced completely to its neutral state, which confirmed that  $\text{NH}_3$  has not enough strength to reduced chemically oxidized **P1** dissolved in  $\text{CH}_2\text{Cl}_2$  solution (**Figure 3.5** and **Table 3.3**). The polymer **P1** could be reversibly switched many times between its half-oxidized and oxidized states.



**Figure 3.4** Changes in optical absorption spectra of chemically obtained polymer **P1** dissolved in  $\text{CH}_2\text{Cl}_2$  solution after the addition of  $2 \mu\text{L}$  (for each spectrum) of  $0.01 \text{ M}$   $\text{SbCl}_5$ .






**Table 3.2** Color changes of **P1** dissolved in  $\text{CH}_2\text{Cl}_2$  solution after the addition of  $\text{SbCl}_5$ .

<b>Oxidation with <math>\text{SbCl}_5</math></b>					
<b>L</b>	51.5	64.2	70.6	75.1	75.8
<b>a</b>	44.0	23.2	10.4	3.36	0.89
<b>b</b>	-5.20	7.36	9.18	8.11	7.03



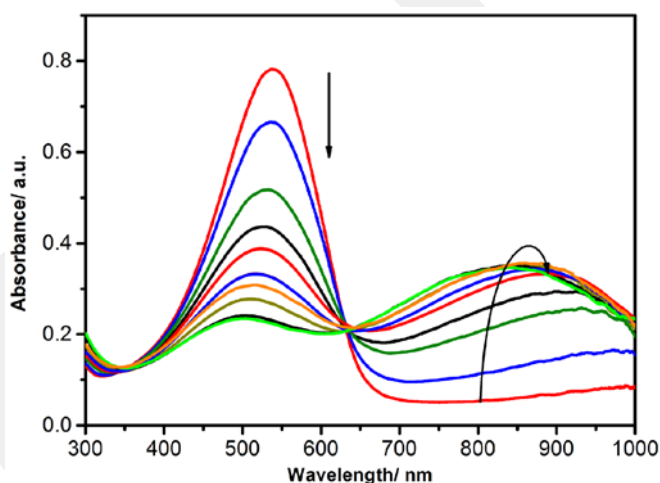
**Figure 3.5** Changes in optical absorption spectra of chemically oxidized **P1** dissolved in  $\text{CH}_2\text{Cl}_2$  solution after addition of 2  $\mu\text{L}$  (for each spectrum) of 0.5 M  $\text{NH}_3$ .

**Table 3.3** Color changes of chemically oxidized **P1** dissolved in  $\text{CH}_2\text{Cl}_2$  solution after the addition of  $\text{NH}_3$ .

<b>Reduction with <math>\text{NH}_3</math></b>					
<b>L</b>	75.8	69.8	64.0	56.2	50.3
<b>a</b>	0.9	8.7	16.7	25.8	28.8
<b>b</b>	7.0	9.2	10.2	12.5	13.3






On the other hand, as shown in **Figure 3.6**, the polymer **P2** solution has a broad  $\pi$ - $\pi^*$  transition band centered at 539 nm with a band gap of 1.96 eV, which is near to its linear hexyl analogue [91].

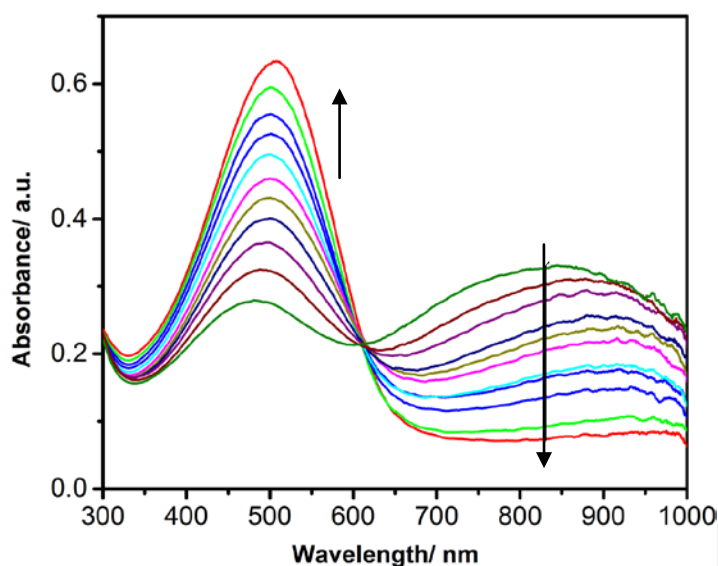
As seen in **Figure 3.6**, by the addition of  $\text{SbCl}_5$ ,  $\pi\text{-}\pi^*$  transition band started to decrease its intensity step by step with a concomitant increase after 700 nm due to the formation of charge carriers. At the end of oxidation, the  $\pi\text{-}\pi^*$  transition nearly disappeared and shifted to 501 nm and the absorption band of the charge carriers reached a maximum intensity. The percent transmittance change at 539 nm was calculated as 28%. Upon oxidation, the color of the neutral **P2** was changed from reddish orange to orange and to transmissive reddish green/green and then to transmissive green/blue during chemical oxidation (**Table 3.4**). Unlike **P1**, by the use of  $\text{NH}_3$ , the polymer can be reduced completely to its neutral state (**Figure 3.7** and **Table 3.5**). The polymer **P2** could be reversibly switched many times between its neutral and oxidized states.



**Figure 3.6** Changes in optical absorption spectra of chemically obtained **P2** dissolved in  $\text{CH}_2\text{Cl}_2$  solution after the addition of 2  $\mu\text{L}$  (for each spectrum) of 0.01 M  $\text{SbCl}_5$ .






**Table 3.4** Color changes of **P2** dissolved in  $\text{CH}_2\text{Cl}_2$  solution after the addition of  $\text{SbCl}_5$ .

<b>Oxidation with <math>\text{SbCl}_5</math></b>					
<b>L</b>	62.9	68.3	74.6	76.6	78.7
<b>a</b>	42.8	30.6	9.8	3.6	-0.5
<b>b</b>	18.1	21.9	18.9	11.0	5.6



**Figure 3.7** Changes in optical absorption spectra of chemically oxidized **P2** dissolved in  $\text{CH}_2\text{Cl}_2$  solution after the addition of  $2 \mu\text{L}$  (for each spectrum) of  $0.5 \text{ M}$   $\text{NH}_3$ .

**Table 3.5** Color changes of chemically oxidized **P2** dissolved in  $\text{CH}_2\text{Cl}_2$  solution after the addition of  $\text{NH}_3$ .

<b>Reduction with <math>\text{NH}_3</math></b>					
<b>L</b>	78.7	74.4	71.8	70.2	67.3
<b>a</b>	-0.5	11.3	18.4	23.4	33.2
<b>b</b>	5.6	17.2	21.0	23.3	24.7

Solubility and processability are one of the most important parameters for electrochromic polymers to be amenable for use in optical devices like electrochromic devices. Therefore, this kind of polymers can be coated on any surfaces via spin coating or spray coating. **Figure 3.8** demonstrated the coating of the polymers **P1** and **P2** on ITO surfaces via a spray coating method. While the color of thin **P2** film in thin film form, for example, is light purple, the thick form is dark purple.

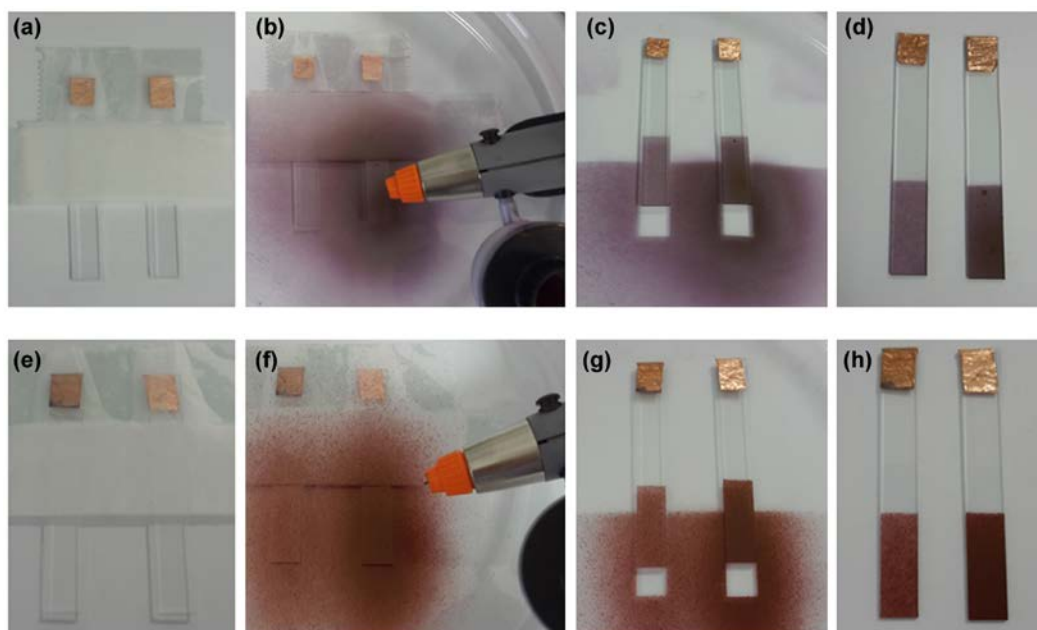


**Figure 3.8** The coating of the polymers (a)-(d) **P1** and (e)-(h) **P2** dissolved in  $\text{CH}_2\text{Cl}_2$  on ITO surfaces via spray coating method.

In order to tune the colors of the polymers **P1** and **P2** by chemical oxidation, the coated polymer films on ITO via the spray coating method were also oxidized and reduced chemically by using  $\text{SbCl}_5$  and  $\text{NH}_3$ , respectively. As shown in **Figure 3.9**, **P1** has a larger  $\pi$ - $\pi^*$  transition band centered at a maximum wavelength of 539 nm than its solution form (524 nm), which can be attributed to the  $\pi$ - $\pi^*$  stacking and increasing conjugation in thin film form. As expected, the calculated band gap of **P1** was found to be as 1.81 eV, also smaller than its solution form (1.90 eV). On the other hand, the color of **P1** was tuned successfully by oxidation and the color changed from brownish red ( $L=47.4$ ,  $a=9.78$ ,  $b=-6.96$ ) to transmissive green/blue ( $L= 59.3$ ,  $a= 2.45$ ,  $b=1.49$ ). By the addition of  $\text{SbCl}_5$ , the optical spectrum of **P1** film started to change as well as its color (**Table 3.2**). The  $\pi$ - $\pi^*$  transition band lost its intensity by shifting to a shorter wavelength. In the same time, the formation of charge carriers confirmed by the appearance of the absorption band beyond 700 nm. After the addition of a certain amount of  $\text{SbCl}_5$ , the polaron band reached a maximum intensity and then decreased due to the formation of another kind of charge carriers called bipolarons. The color of the neutral polymer was changed from purple to transmissive blue when oxidized (**Figure 3.9**). On the other hand, the polymer film

couldn't be reduced completely to its neutral state by the use of  $\text{NH}_3$  (**Figure 3.10**), which may be due to the reducing strength of  $\text{NH}_3$  or the polymer chain stacking in film for when compared to the solution.

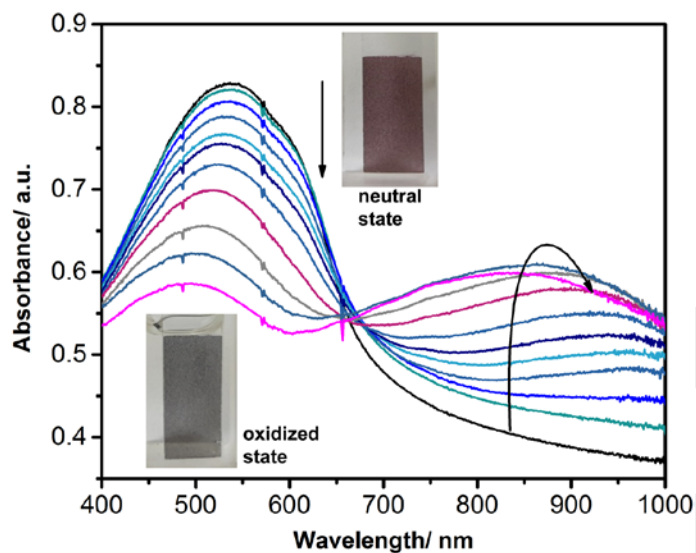


**Figure 3.9** Changes in optical absorption spectra of coated **P1** on ITO in acetonitrile after addition of 2  $\mu\text{L}$  (for each spectrum) of 0.1 M  $\text{SbCl}_5$ . Inset: Colors of the film at different oxidation states.

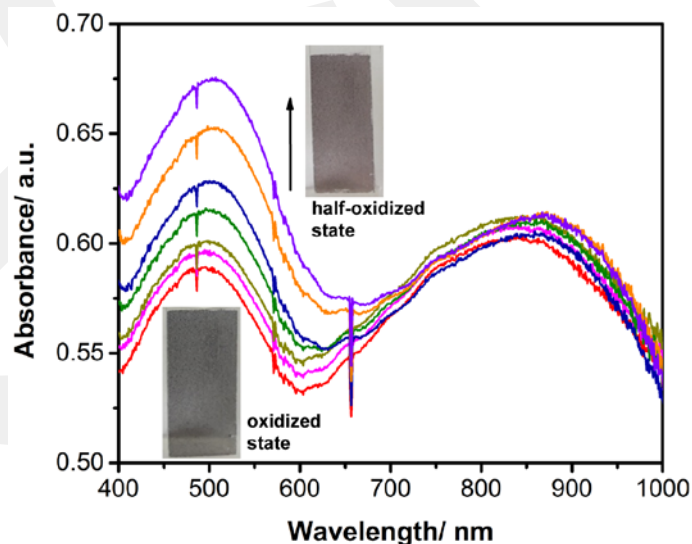


**Figure 3.10** Changes in optical absorption spectra of chemically oxidized **P1** on ITO in acetonitrile solution after addition of 2  $\mu\text{L}$  (for each spectrum) of 0.5 M  $\text{NH}_3$ . Inset: Colors of the film at different oxidation states.

Like **P1**, in order to tune the colors of the polymer film **P2** by chemical oxidation, the coated polymer film **P2** on ITO was oxidized and reduced chemically by using  $\text{SbCl}_5$  and  $\text{NH}_3$ , respectively. **P2** has a  $\pi$ - $\pi^*$  transition band at 537 nm with a band gap of 1.92 eV, which is somewhat smaller than its solution form (1.96 eV). The color of **P2** was changed from brownish red ( $L=50.0$ ,  $a=33.8$ ,  $b=14.5$ ) to transmissive blue ( $L=62.7$ ,  $a=0.82$ ,  $b=8.38$ ). By the addition of  $\text{SbCl}_5$ , the intensity of the  $\pi$ - $\pi^*$  transition band started to decrease and the appearance of the absorption band beyond 650 nm confirmed the formation of new charge carriers (**Figure 3.11**). On the other hand, unlike its solution form, the polymer film **P2** couldn't be reduced completely to its neutral state (**Figure 3.12**), which may be due to the polymer chain stacking in film form when compared to the solution.

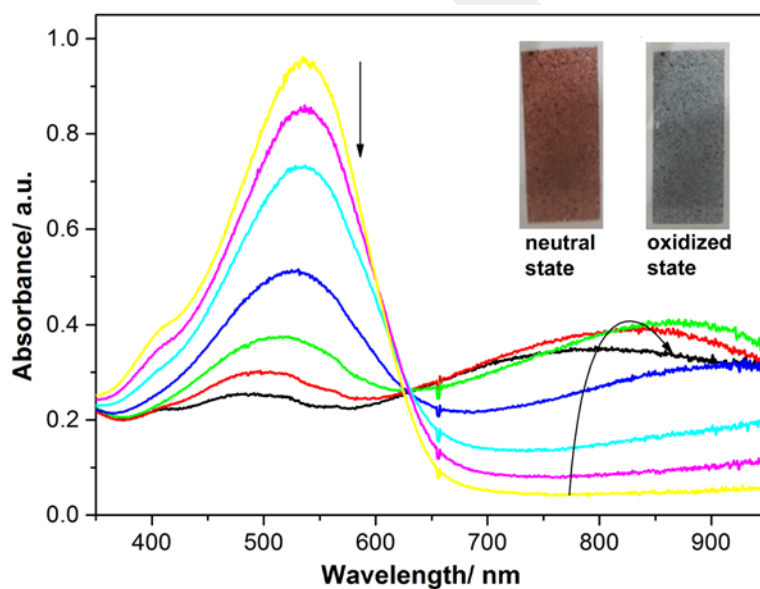


**Figure 3.11** Changes in optical absorption spectra of coated **P2** on ITO in acetonitrile after addition of 2  $\mu\text{L}$  (for each spectrum) of 0.1 M  $\text{SbCl}_5$ . Inset: Colors of the film at different oxidation states.

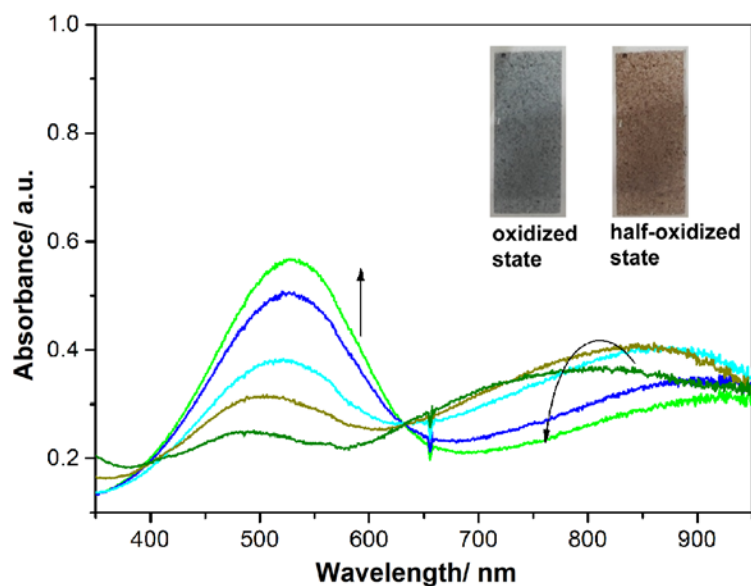


**Figure 3.12** Changes in optical absorption spectra of chemically oxidized **P2** on ITO in acetonitrile solution after addition of 2  $\mu\text{L}$  (for each spectrum) of 0.5 M  $\text{NH}_3$ . Inset: Colors of the film at different oxidation states.

### 3.3 Opto-Electrochemical Studies

In order to study the opto-electrochemical properties of the polymer films, the redox behaviours of the films coated on Pt electrodes by using a drop casting method were investigated by using cyclic voltammetry in an electrolyte solution of 0.1 M TBAH dissolved in acetonitrile. The polymer films couldn't show any redox behaviour during cathodic scan from 0.0 V to -1.5 V, whereas they exhibited a well-defined oxidation peak at 1.0 V for **P1** and 1.4 V for **P2** during anodic scan and their reduction peaks appeared at 0.9 V during reverse scan at a scan rate of 100 mV/s. As shown in **Figure 3.13** and **Figure 3.14**, the polymer films **P1** and **P2** are firmly adhered to the electrode surface since the redox couple current intensified with increasing scan rate. Also, the currents increased linearly as a function of scan rate, which confirms that the redox behaviour of well-adhered electroactive polymer films are nondiffusional process.

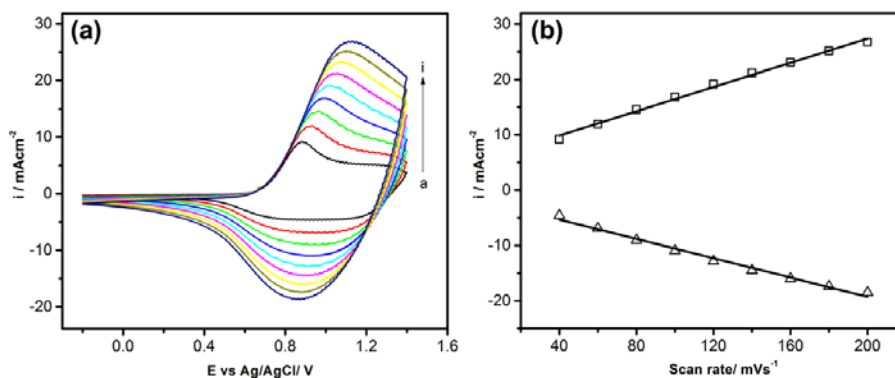


**Figure 3.13** (a) Scan rate dependence of the polymer film **P1** coated on Pt electrode in 0.1 M TBAH/acetonitrile solution at different scan rates (mV/s), a: 40, b: 60, c: 80, d: 100, e: 120, f: 140, g: 160, h: 180 and i: 200. (b) Relationship of anodic and cathodic current peaks as a function of scan rate in 0.1 M TBAH/acetonitrile solution.

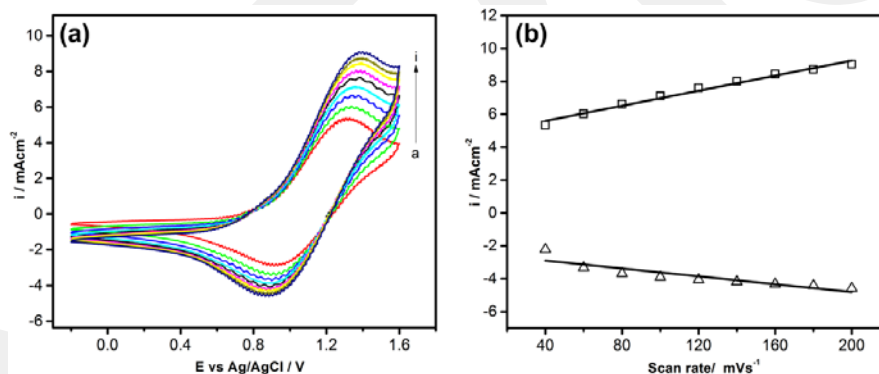


**Figure 3.14** (a) Scan rate dependence of the polymer film **P2** coated on Pt electrode in 0.1 M TBAH/acetonitrile solution at different scan rates (mV/s), a: 40, b: 60, c: 80, d: 100, e: 120, f: 140, g: 160, h: 180 and i: 200. (b) Relationship of anodic and cathodic current peaks as a function of scan rate in 0.1 M TBAH/acetonitrile solution.

After the determination of working potential range for the polymer films, the optical changes in the spectra were determined under applied external potentials. **Figure 3.15** exhibited the changes in the absorption spectrum of the polymer **P1**. As expected, upon moving from 0.0 V to 1.5 V, the  $\pi$ - $\pi^*$  transition band started to lose its intensity with a concomitant appearance of a new broad band centered at 800 nm,

which could be attributed to the formation of polaron charge carriers. During further oxidation, the transition band nearly disappeared and beyond 950 nm a new absorption band begins to intensify, indicating the formation of bipolaron charge carriers. These absorbance variations occurred around an isosbestic point at 649 nm, indicating the coexistence of only two phases. The application of even more anodic potentials couldn't change the position of the isosbestic point. The color of the thin polymer film is dark purple (L=54.2, a=5.94, b=-12.4) when neutralized and transmissive blue (L=65.5, a=3.08, b=0.40) when oxidized. Inset of **Figure 3.15** exhibited the color changes of **P1** film during p-doping.

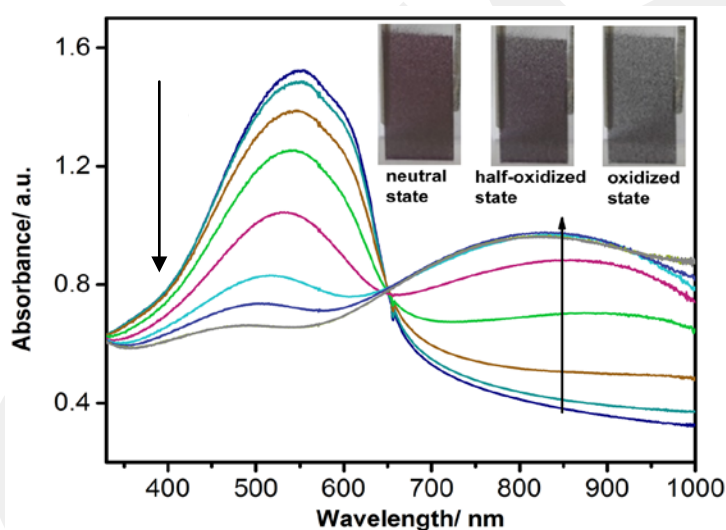


**Figure 3.15** Optical absorption spectra of **P1** film on ITO in 0.1 M TBAH/acetonitrile at various applied potentials upon moving from 0.0 V to 1.5 V.

On the other hand, as shown in **Figure 3.16**, the  $\pi$ - $\pi^*$  transition band of **P2** film at 537 nm disappeared completely at the end of oxidation. During oxidation upon moving from 0.0 V to 1.5 V, like **P1** film, the formation of charge carriers was confirmed by the appearance of a new broad band centered at 800 nm and also towards at the end of oxidation the appearance of a new band beyond 950 nm confirmed the formation of bipolaron charge carriers. In addition, **P2** exhibited a multichromic behaviour upon oxidation: brownish red, brown, light brown, transmissive gray and transmissive blue. Inset of **Figure 3.16** exhibited the color changes of **P2** film upon oxidation.

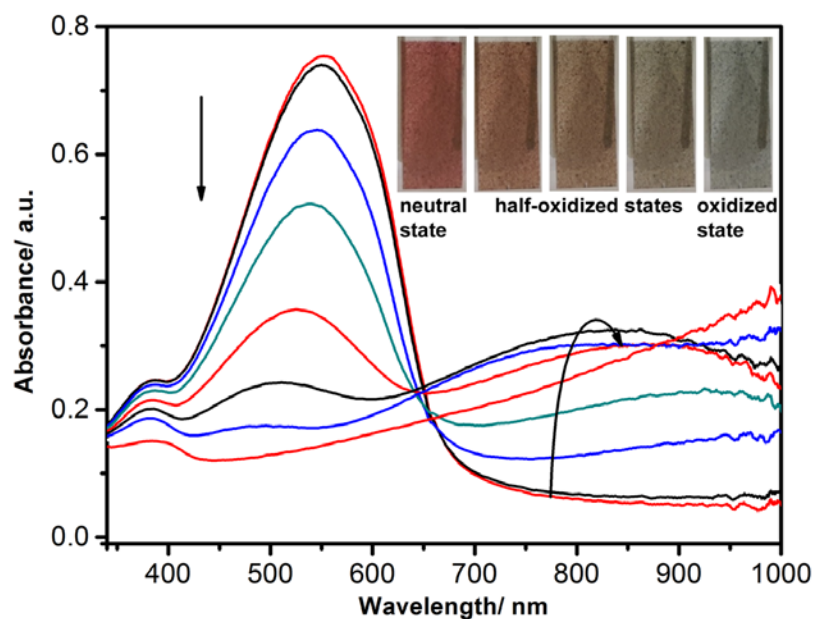


**Figure 3.16** Optical absorption spectra of **P2** film on ITO in 0.1 M TBAH/acetonitrile at various applied potentials upon moving from 0.0 V to 1.5 V.

### 3.4 Thermal Properties

The thermal stabilities of the polymers were investigated by the TGA analysis. The TGA thermograms of the polymers are shown in **Figure 3.17**. First of all, the polymers **P1** and **P2** started to lose their weights slowly and continuously after 100 and 200 °C, respectively. The maximum decomposition temperatures are at 406 °C for **P1** and 466 °C for **P2**, these losses can be attributed to the alkyl chains and the polymers retained 53.4% and 38.7% of their weights at 900 °C, respectively.

On the other hand, DSC thermograms of polymers **P1** and **P2** did not show any glass transition temperature and crystallization/melting transitions. Unfortunately, the DSC thermograms showed nearly flat lines with no changes and as a result no glass transition temperatures of polymers were observed in the measured temperature from 25 °C to 200 °C.

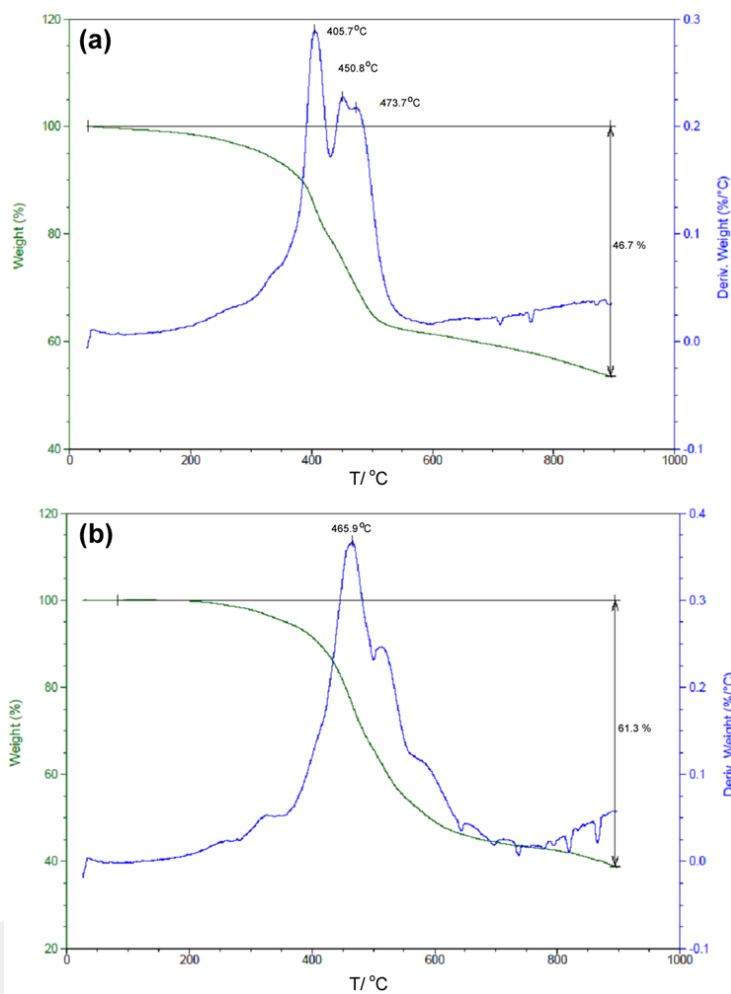


**Figure 3.17** TGA thermograms of (a) **P1** and (b) **P2**.

### 3.5 Electrochromic Devices

Electrochromic device based on **P1** showed a reversible response between a potential range from -1.8 to +1.8 V (**Figure 3.18**). The device has a maximum oxidation wave at 0.70 V and a maximum reduction wave at 0.34 V at a scan rate of 100 mV/s. At -1.8V, the color of the device was dark blue/violet and it changed to dark brown upon moving from -1.8 V to +1.8 V (**Figure 3.19**). Upon oxidation, the intensity of the absorption band at 555 nm, attributed the neutral PEDOT, was decreased and a new band beyond 700 nm appeared due to the reduced state of **P1** layer.

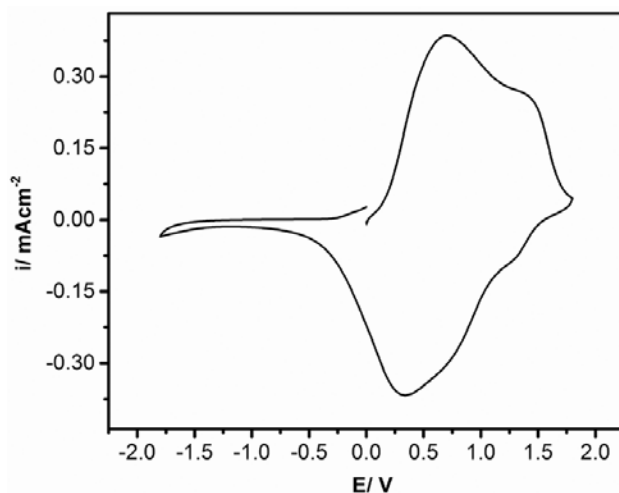


**Figure 3.18** Cyclic voltammogram of PEDOT/**P1** based electrochromic device at a scan rate of 100 mV/s between -1.8 V and 1.8 V.

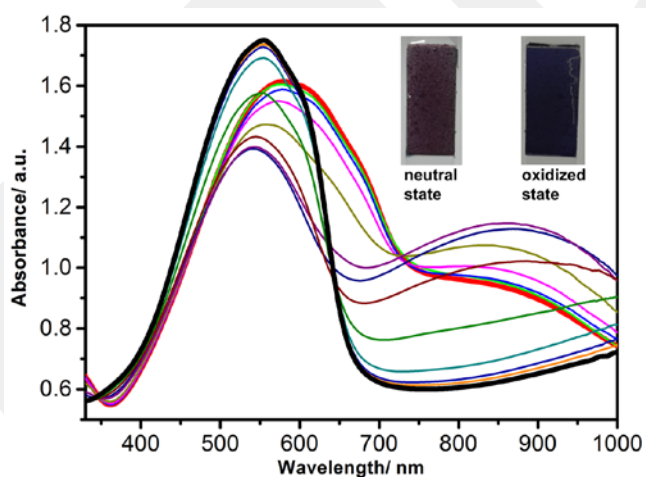


**Figure 3.19** Optical characterization of PEDOT/**P1** electrochromic device by applying different potentials between -0.1 V and 1.8 V. The colors of device at -1.0 V and 1.8 V. PEDOT was used as a cathode electrode.

On the other hand, like **P1**, the electrochromic device based on **P2** showed a reversible response between a potential range from -1.8 to +1.8 V (**Figure 3.20**). While the device exhibited two oxidation peak at 0.91 V and 1.51 V, a maximum reduction wave was appeared at 0.72 V with a shoulder at 1.34 V. The color of the device was dark blue/violet at -1.8 V, and the color was changed to dark brown at +1.8 V (**Figure 3.21**). During electrochemical study, the absorption band at 505 nm

preserved its intensity, but a new band beyond 700 nm appeared and intensified by increasing applied potential, which can be attributed to the reduced state of **P2** layer.

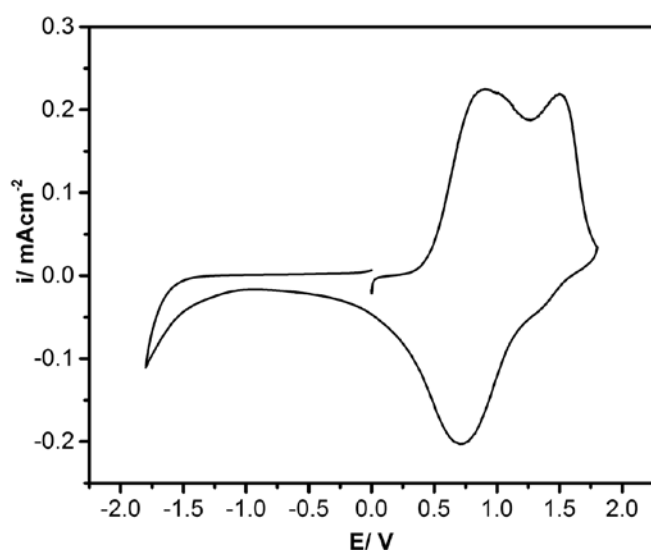


**Figure 3.20** Cyclic voltammogram of PEDOT/**P2** based electrochromic device at a scan rate of 100 mV/s between -1.8 V and 1.8 V.

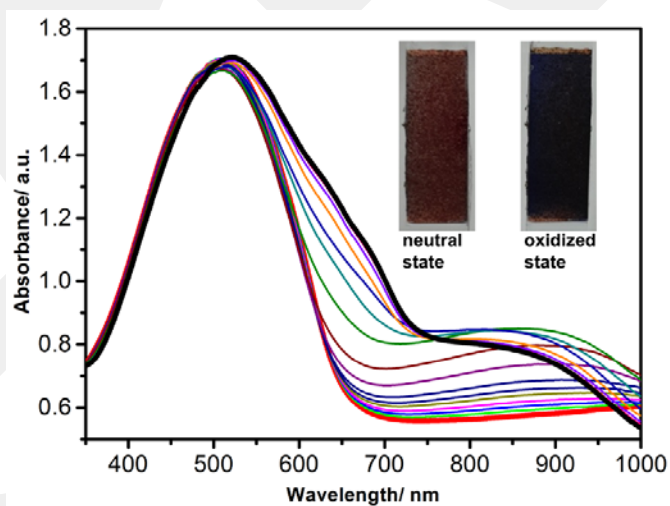


**Figure 3.21** Optical characterization of PEDOT/**P2** electrochromic device by applying different potentials between -1.8 V and 1.8 V. The colors of device at -1.0 V and 1.8 V. PEDOT was used as a cathode electrode.

## CHAPTER 4

### CONCLUSION

Two new thienosilole based soluble polymers bearing thiophene (**P1**) and bithiophene (**P2**) units were successfully synthesized via Stille Coupling reaction. The presence of 2-ethylhexyl alkyl chain on the thienosilole ring in the corresponding polymers resulted in solubility in commonly used solvents. The polymers were characterized by using NMR, GPC, SEM and TGA techniques. The weight average molecular weights of the polymers **P1** and **P2** were found to be as 70977 with a PDI of 2.30 and 110439 with a PDI of 1.42, respectively. The band gaps of polymers were found to be as 1.81 eV for **P1** and 1.92 eV for **P2**.

On the other hand, the polymers exhibited fluorescent property. The polymers dissolved in toluene have maximum emission bands at 634 nm for **P1** and 613 for **P2**. On this basis, it can be easily concluded that these polymers can be amenable for use in various fields such as light emitting diodes, organic lasers and electroluminescent materials.

The polymers exhibited both chemochromic and electrochromic properties. While the colors of the neutral polymer films are purple for **P1** and reddish brown for **P2**, both polymers are transparent sky blue at their oxidized states. Also, the electrochromic device applications showed that they can be good candidates for optoelectronic applications.

## REFERENCES

- [1] Letheby, H., 1862. On the Production of a Blue Substance by the Electrolysis of Sulphate of Aniline. *J. Chem. Soc.*, 15, 161-163.
- [2] Shirakawa, H., Lewis, E.J., MacDiarmid, A.G., Chiang, C.K., Heeger, A.J. 1977. Synthesis of electrically conducting organic polymers: halogen derivatives of polyacetylene,  $(CH)_x$ . *J. Chem. Soc., Chem. Commun.*, 578-580.
- [3] Karzazi, Y. 2014. Organic Light Emitting Diodes: Devices and applications. *J. Mater. Environ. Sci.*, 5, 2028-2508.
- [4] Greenham, C., Moratti, S.C., Bradley, D.D.C., Friend, R.H., Holmes, A.B. 1993. Efficient light-emitting diodes based on polymers with high electron affinities. *Nature*, 365, 628-630.
- [5] Friend, R.H., Gymer, R.W., Holmes, A.B., Burroughes, J.H., Marks, R.N., Taliani, D.D.C., DosSantos, D.A., Bredas, J.L., Logdlund, M., Salaneck, W.R. 1999. Electroluminescence in conjugated polymers. *Nature*, 397, 121-127.
- [6] Ho, P.K.H., Kim, J.S., Burroughes, J.H., Becker, H., Li, S.Y., Brown, T.M., Cacialli, F., Friend, R.H. 2000. Molecular-scale interface engineering for polymer light-emitting diodes. *Nature*, 404, 481-484.
- [7] Sariciftci, N.S., Smilowitz, L., Heeger, A.J., Wudl, F. 1992. Photoinduced electron transfer from a conducting polymer to buckminsterfullerene. *Science*, 258, 1474-1476.
- [8] Schmidt-Mende, L., Fechtenkotter, A., Mullen, K., Moons, E., Friend, R.H., Mackenzie, J.D. 2001. Self-organized discotic liquid crystals for high-efficiency organic photovoltaics. *Science*, 293 1119-1122.
- [9] Liscio, A., De Luca, G., Nolde, F., Palermo, V., Mullen, K., Samori, P. 2008. Photovoltaic charge generation visualized at the nanoscale: a proof of principle. *J. Am. Chem. Soc.*, 130, 780-781.
- [10] Frechet, J.M.J., Thompson, B.C. 2008. Polymer-fullerene composite solar cells. *Angew. Chem. Int. Ed.*, 47, 58-77.

- [11] Schwendeman, I., Hickman, R., Sonmez, G., Schottland, P., Zong, K., Welsh, D., Reynolds, J.R. 2002. Enhanced Contrast Dual polymer electrochromic Devices. *Chem. Mater.*, 14, 3118-3122.
- [12] Meng, H., Tucker, D., Chaffins, S., Chen, Y., Helgeson, R., Dunn, B., Wudl, F. 2003. An unusual electrochromic device based on a new low-bandgap conjugated polymer. *Adv. Mater.*, 15, 146-149.
- [13] Cihaner, A., Algi, F. 2008. Processable rainbow mimic fluorescent polymer and its unprecedented coloration efficiency in electrochromic device. *Electrochim. Acta*, 53, 2574-2578.
- [14] Pennisi, A., Simone, F., Barletta, G., Di Marco, G., Lanza, L. 1999. Preliminary test of a large electrochromic window. *Electrochim. Acta*, 44, 3237-3243.
- [15] Rauh, D.R. 1999. Electrochromic windows: an overview. *Electrochim. Acta*, 44, 3165-3176.
- [16] Cooke, G., Garety, J., Mabruk, S., Rotello, V., Surpateanu, G., Woisel, P. 2004. The electrochemically tuneable recognition properties of an electropolymerised flavin derivative. *Chem. Commun.*, 2722-2723.
- [17] Asil, D., Cihaner, A., Önal, A.M. 2009. A Glow in the Dark: Synthesis and Electropolymerization of a Novel Chemiluminescent Terthienyl System. *Chem. Commun.*, 3, 307-309.
- [18] Asil, D., Cihaner, A., Algi, F., Önal, A.M. 2010. A diverse-stimuli responsive chemiluminescent probe with luminol scaffold. *Electroanalysis*, 22, 2254-2260.
- [19] Usta, H., Facchetti, A., Marks, T.J. 2008. Air-Stable, Solution-Processable n-Channel and Ambipolar Semiconductors for Thin-Film Transistors Based on the Indenofluorenebis (dicyanovinylene) Core. *J. Am. Chem. Soc.*, 130, 8580-8581.
- [20] Chen, Z., Lemke, H., Albert-Seifried, S., Caironi, M., Nielsen, M.M., Heeney, M., Zhang, W., McCulloch, I., Sringhaus, H. 2010. High Mobility Ambipolar Charge Transport in Polyselenophene Conjugated Polymers. *Adv. Mater.*, 22, 2371-2375.

- [21] McCullough R.D., Renae, D.L., Manikandan J., Deborah L.A. 1993. Design, Synthesis, and Control of Conducting Polymer Architectures: Structurally Homogeneous Poly(3-alkylthiophenes). *J. Org. Chem.*, 58, 904-912.
- [22] John, R.N., Brett, P.F., Xiaoxing, W., Jonathon, T., Gunn, S.L. 2010. Stille cross-coupling reactions of aryl mesylates and tosylates using a biarylphosphine based catalyst system. *Heterocycles*, 80, 1215-1226.
- [23] Nicolaou, K. C., Paul, G. Bulger, Sarlah, David 2005. Palladium-Catalyzed Cross-Coupling Reactions in Total Synthesis. *Angew.Chem. Int. Ed.*, 44, 4442-4489.
- [24] Espinet, P., Echavarren, M. 2004. The Mechanisms of the Stille Reaction. *Angew. Chem. Int. Ed.*, 43, 4704-4734.
- [25] Allen, J.B., Gyorgy, I., Fritz, S. 2012. *Electrochemical Dictionary*. Second edition, Springer.
- [26] Wei, Y., Cheung, C., Jing, C., Guang-Way, T., Kesyin, J. 1991. Electrochemical Polymerization of Thiophenes in the Presence of Bithiophene or Terthiophene: Kinetics and Mechanism of the Polymerization. *Chem. Mater.*, 3, 888-897.
- [27] Suarez-Herrera, M.F. 2010. *Electrochemistry-conducting polymers*, Encyclopedia of Life Support Systems (EOLSS).
- [28] Pron, A., Gawrys, P., Zagorska, M., Djuradoa, D., Demadrillea, R. 2010. Electroactive materials for organic electronics: preparation strategies, structural aspects and characterization techniques. *Chem. Soc. Rev.*, 39, 2577-2632.
- [29] Medlej, H., Awada, H., Abbas, M., Wantz, G., Bousquet, A., Grelet, E., Hariri, K., Hamieh, T., Hiorns, R.C., Dagrón-Lartigau, C. 2013. Effect of spacer insertion in a commonly used dithienosilole/benzothiadiazole-based low band gap copolymer for polymer solar cells. *Eur. Polym. J.*, 49, 4176-4188.
- [30] Thomas, C.A., 2002. Donor-acceptor methods for band gap reduction in conjugated polymers: the role of electron rich donor heterocycles. PhD Thesis.
- [31] Bresse, F., Remond, G., Akamatsu, B. 1996. *Cathodoluminescence Microscopy and Spectroscopy of Semiconductors and Wide Bandgap Insulating Materials*. Springer *Mikrochim. Acta*, 13, 135-166.

- [32] Lee, Y., Lee, M., Sadki, S., Tsuie, B., Reynolds, J.R. 2002. A New Narrow Band Gap Electroactive Silole Containing Polymer. *Mol. Cryst. Liq. Cryst.*, 377, 289-292.
- [33] Uchida, M.T., Izumikawa, T.N., Yamaguchi, S., Tamao, K. 2001. Structural Optimization of 2,5-Diarylsiloles as Excellent Electron-Transporting Materials for Organic Electroluminescent Devices. *Chem. Mater.* 13, 2680-2683.
- [34] Luo, J., Xie, Z., Lam, W.Y., Cheng, L., Chen, H., Qiu, C., Kwok, H.S., Zhan, X., Liu, Y., Zhu, D., Tang, B.Z. 2001. Aggregation-induced emission of 1-methyl-1,2,3,4,5-pentaphenylsilole. *Chem. Commun.*, 1740-1741.
- [35] Adachi, H., Yasuda, T., Sanji, H., Sakurai, K., Okita, J. 2000. Organic Electroluminescence of Silole-Incorporated Polysilane. *J. Luminescence*, 87, 1174-1176.
- [36] Chen, J.W., Law, C.C.W., Lam, J.W.Y., Dong, Y.P., Lo, S.M.F., Williams, I.D., Zhu, D.B., Tang, B.Z. 2003. Synthesis, Light Emission, Nanoaggregation, and Restricted Intramolecular Rotation of 1,1-Substituted 2,3,4,5-Tetraphenylsiloles. *Chem. Mater.*, 15, 1535-1546.
- [37] Chen, J.W., Xie, Z., Lam, J.W.Y., Law, C.C.W., Tang, B.Z. 2003. Silole-Containing Polyacetylenes. Synthesis, Thermal Stability, Light Emission, Nanodimensional Aggregation, and Restricted Intramolecular Rotation. *Macromolecules*, 36, 1108-1117.
- [38] Nguyen, H.T., Huong, V.T.T., Nguyen, M.T. 2012. Silole-based oligomers as electron transport materials. *Chem. Phys. Lett.*, 550, 33-40.
- [39] Zhenguo, W., Jie, Z., Li, Y., Peng, Q. 2014. Low band-gap copolymers derived from fluorinated isoindigo and dithienosilole: synthesis, properties and photovoltaic applications. *Polym. Chem.*, 5, 4984-4992.
- [40] Yamaguchi, S. 1996. Design of novel  $\sigma^*-\pi^*$  conjugated polysilanes *Synth. Met.*, 82, 149-153.
- [41] Hong, S.Y., Song, J.M. 1997. Geometrical and electronic-structures of new  $\pi$ -conjugated pyrrole-nonheterocycle and furan-nonheterocycle copolymers. *Chem. Mater.*, 9, 297-303.

- [42] Ohshita, J. 2009. Conjugated Oligomers and Polymers Containing Dithienosilole Units, *Macromol. Chem. Phys.*, 210, 1360-1370.
- [43] Tamao, K., Yamaguchi, S., 2000. New Type of Polysilanes: Poly(1,1-silole)s. *J. Organomet. Chem.*, 611, 5-11.
- [44] Yamaguchi, S., Tamao, K., 1998. Silole-Containing sigma- and pi-Conjugated Compounds. *J. Chem. Soc., Dalton. Trans.* 22, 3693-3702.
- [45] Yamaguchi, S., Tamao, K. 1996. Theoretical Study of the Electronic Structure of 2,2'-Bisilole in Comparison with 1,1'-Bi-1,3-cyclopentadiene:  $\sigma^*$ - $\pi^*$  Conjugation and a Low-Lying LUMO as the Origin of the Unusual Optical Properties of 3,3',4,4'-Tetraphenyl-2,2'-bisilole. *Bull. Chem. Soc. Jpn.*, 69, 2327-2334.
- [46] Yamaguchi, S., Tamao, K., 2001. Polysiloles and Silole-Containing Polymers Supplement Si: *Organic Silicon Compounds*. 3, 641-694.
- [47] Yamaguchi, S., Endo, T., Uchida, M., Izumizawa, T., Furukawa, K., Tamao, K. 2000. Toward New Materials for Organic Electroluminescent Devices: Synthesis, Structures, and Properties of a Series of 2, 5-Diaryl-3,4-diphenylsiloles. *Chem. Eur. J.*, 6, 1683-1692.
- [48] Ohshita, J., Iida, T., Kanehara, K., Adachi, A., Okita, K. 2003. Synthesis and Properties of Silicon-Bridged Bithiophenes and Application to EL Devices. *Synth. Met.*, 137, 1007-1008.
- [49] Ohshita, J., Nodono, M., Kai, H., Watanabe, T., Kunai, A., Komaguchi, K., Shitotani, M., Adachi, A., Okita, K., Harima, Y. 2000. Synthesis and properties of alternating polymers containing 2,6-diaryldithienosilole and organosilicon units. *Macromol. Chem. Phys.*, 201, 851-857.
- [50] Yamashita, K., Ishikawa, M. 1999. Synthesis and Optical, Electrochemical, and Electron-Transporting Properties of Silicon-Bridged Bithiophenes. *Organometallics*, 18, 1453-1459.
- [51] Tamao, K., Uchida, M., Izumizawa, T., Furukawa, K., Yamaguchi, S. 1996. Silole Derivatives as Efficient Electron Transporting Materials. *J. Am. Chem. Soc.*, 118, 11974-11975.

- [52] Ohshita, J., Kai, H., Takata, A., Iida, T., Kunai, A., Ohta, N., Komaguchi, K., Shiotani, M., Adachi, A., Sakamaki, K., Okita, K. 2001. Effects of Conjugated Substituents on the Optical, Electrochemical, and Electron-Transporting Properties of Dithienosiloles. *Organometallics*, 20, 4800-4805.
- [53] Chan, K.L., McKiernan, M.J., Towns, C.R., Holmes, A.B. 2005. Poly(2,7-dibenzosilole): A Blue Light Emitting Polymer. *J. Am. Chem. Soc.*, 127, 7662-7663.
- [54] Kim, W., Palilis, L.C., Uchida, M., Kafafi, Z.H. 2004. Efficient Silole-Based Organic Light-Emitting Diodes Using High Conductivity Polymer Anodes. *Chem. Mater.*, 16, 4681-4686.
- [55] Liu, M.S., Luo, J.D., Jen, A.K.Y. 2003. Efficient Green-Light-Emitting Diodes from Silole-Containing Copolymers *Chem. Mater.*, 15, 3496-3500.
- [56] Murata, H., Kafafi, Z.H., Uchida, M. 2002. Efficient organic light-emitting diodes with undoped active layers based on silole derivatives. *Appl. Phys. Lett.*, 80, 189-191.
- [57] Huanli, D., Jiang L., Hu, W. 2012. Interface engineering for high-performance organic field-effect transistors. *Phys. Chem. Chem. Phys.*, 14, 14165-14180.
- [58] Ohshita, J., Lee, K.H., Kunugi, Y., Kunai, A. 2006. Synthesis of  $\pi$ -Conjugated Oligomers Containing Dithienosilole Units. *Organometallics*, 25, 1511-1516.
- [59] Fei, Z., Kim, Jeremy Smith, Ester Buchaca Domingo, Thomas D. Anthopoulos, Natalie Stingel J.S., Watkins, S.E., Kim, J.S., Heeney, M. 2011. A low band gap copolymer of dithienogermole and 2,1,3-benzothiadiazole by Suzuki polycondensation and its application in transistor and photovoltaic cells. *J. Mater. Chem.*, 21, 16257-16263.
- [60] Sirringhaus, H. 2014. Organic Field-Effect Transistors: The Path Beyond Amorphous Silicon. *Adv. Mater.*, 26, 1319-1335.
- [61] Muccini, M. 2006. A bright future for organic field-effect transistors. *Nature Mater.*, 5, 605-613.
- [62] Sirringhaus, H. 2005. Device Physics of Solution-Processed Organic Field-Effect Transistors. *Adv. Mater.*, 17, 2411-2425.

- [63] Yuji, Y., Kei, N., Yamada, H., Matsushige, K. 2012. Organic field-effect transistors with molecularly doped polymer gate buffer layer. *Synth. Met.*, 162, 1887-1893.
- [64] Huanli, D., Wang, C., Hu, W. 2010. High performance organic semiconductors for field-effect transistors. *Chem. Commun.*, 46, 5211-5222.
- [65] Ohshita, J., Kimura, K., Lee, K., Kunai, H.A., Kwak, Y.W., Son, E.C., Kunug, Y. 2007. Synthesis of silicon-bridged polythiophene derivatives and their applications to EL device materials. *J. Polym. Sci., Part A: Polym. Chem.*, 45, 4588-4596.
- [66] Ribierre, J.C., Takaishi, K., Muto, T., Aoyama, T. 2011. Flexible organic field-effect transistors and complementary inverters based on a solution-processable quinoidal oligothiophene derivative. *Opt. Mater.*, 33, 1415-1418.
- [67] Wang, J.Y., Hau, S.K., Yip, H.L., Davies, J.A., Chen, K.S., Zhang, Y., Sun, Y., Jen, A.K.Y. 2011. Benzobis(silolothiophene)-Based Low Bandgap Polymers for Efficient Polymer Solar Cells. *Chem. Mater.*, 23, 765-767.
- [68] Lu, G., Usta, H., Risko, C., Wang, L., Facchetti, A., Ratner, M.A., Marks, T.J. 2008. Synthesis, Characterization, and Transistor Response of Semiconducting Silole Polymers with Substantial Hole Mobility and Air Stability. *Experiment and Theory. J. Am. Chem. Soc.*, 130, 7670-7685.
- [69] Sun, Y., Liu, Y., Zhu, D. 2005. Advances in organic field-effect transistors. *J. Mater. Chem.*, 15, 53-65.
- [70] Askari, M.B. 2014. Comparison of organic solar cells and inorganic solar cells. *IJRSE*, 3, 53-58.
- [71] Servaites, J.D., Ratner, M.A., Marks, T.J. 2011. Organic solar cells: A new look at traditional models. *Energy Environ. Sci.*, 4, 4410-4422.
- [72] Lin, L.Y., Chen, Y.H., Huang, Z.Y., Lin, H.W., Chou, S.H., Lin, F., Chen, C.W., Liu, Y.H., Wong, K.T. 2011. A Low-Energy-Gap Organic Dye for High-Performance Small-Molecule Organic Solar Cells. *J. Am. Chem. Soc.*, 133, 15822-15825.

- [73] Liao, L., Dai, L., Smith, A., Michael, D., Lu, J., Ding, J., Tao, Y. 2007. Photovoltaic-Active Dithienosilole-Containing Polymers. *Macromolecules*, 40, 9406-9412.
- [74] Fei, Z., Kim, J.S., Smith, J., Buchaca, D.E., Anthopoulos, T.D., Stingelin, N., Watkins, S.E., Kim, J.S., Heeney, M. 2011. A low band gap co-polymer of dithienogermole and 2,1,3-benzothiadiazole by Suzuki polycondensation and its application in transistor and photovoltaic cells. *J. Mater. Chem.*, 21, 16257-16263.
- [75] Wang, E.G., Wang, L., Lan, L., Luo, F.C., Zhuang, W.L., Peng, J.B., Cao, Y. 2008. High-performance polymer heterojunction solar cells of a polysilafuorene derivative. *Appl. Phys. Lett.*, 92, 033307-1-033307-3.
- [76] Feron, K., Belcher, W.J., Fell, C.J., Dastoor, P.C. 2012. Organic Solar Cells: Understanding the Role of Forster Resonance Energy Transfer. *Int. J. Mol. Sci.*, 13, 17019-17047.
- [77] Travis, L., Venkataraman, B.D. 2006. Organic solar cells: An overview focusing on active layer morphology. *Photosynth. Res.*, Springer., 87, 73-81.
- [78] Hoppea, H., Sariciftci, N.S. 2004. Organic solar cells: An overview. *J. Mater. Res.*, 19, 1924-1945.
- [79] Ke, J.C., Wang, Y.H., Chen, K.L., Huang, C.J. 2015. Effect of organic solar cells using various sheet resistances of indium tin oxide and different cathodes: Aluminum, silver. *Synth. Met.*, 201, 25-29.
- [80] Ding, J., Song, N., Li, Z. 2010. Synthesis, characterization and photovoltaic applications of a low band gap polymer based on s-tetrazine and dithienosilole. *Chem. Commun.*, 46, 8668-8670.
- [81] Ohshita, J., Kimura, K., Lee, K.H., Kunai, A., Kwak, Y.W., Son, E.C., Kunug, Y.J. 2007. Synthesis of Silicon-Bridged Polythiophene Derivatives and Their Applications to EL Device Materials. *J. Polym. Sci.: Part A: Polym. Chem.*, 45, 4588-4596.
- [82] Ashraf, R.S., Chen, Z.Y., Leem, D.S., Bronstein, H., Zhang, W.M., Schroeder, B., Geerts, Y., Smith, J., Watkins, S., Anthopoulos, T.D., Sirringhaus, H., de Mello J.C., Heeney, M., McCulloch, I. 2011. Silaindacenodithiophene Semiconducting

Polymers for Efficient Solar Cells and High-Mobility Ambipolar Transistors. *Chem. Mater.*, 23, 768-770.

[83] Zhang, Y., Zou, J., Yip, H.L., Chen, K.S., Zeigler, D.F., Sun, Y., Jen, A.K.Y. 2011. Indacenodithiophene and Quinoxaline Based Conjugated Polymers for Highly Efficient Polymer Solar Cells. *Chem. Mater.*, 23, 2289-2291.

[84] Joji, O., Mitsunori, N., Kai, H., Watanabe, T., Kunai, A., Komaguchi, K., Shiotani, M., Adachi, A., Okita, K., Harima, Y., Yamashita, K., Ishikawa, M. 1999. Synthesis and Optical, Electrochemical, and Electron-Transporting Properties of Silicon-Bridged Bithiophenes. *Organometallics*, 18, 1453-1459.

[85] Hou, J., Chen, H.Y., Zhang, S., Li, G., Yang, Y. 2008. Synthesis, Characterization, and Photovoltaic Properties of a Low Band Gap Polymer Based on Silole-Containing Polythiophenes and 2,1,3-Benzothiadiazole. *J. Am. Chem. Soc.*, 130, 16144-16145.

[86] Carsten, B., He, F., Son, H.J., Xu, T., Yu, L. 2011. Stille Polycondensation for Synthesis of Functional Materials. *Chem. Rev.*, 111, 1493-1528.

[87] Zhang, M., Guo, X., Zhang, Z.G., Li, Y. 2011. D-A copolymers based on dithienosilole and phthalimide for photovoltaic Materials. *Polymer*, 52, 5464-5470.

[88] Yip, H.L., Jen, A.K.Y. 2012. Recent advances in solution-processed interfacial materials for efficient and stable polymer solar cells. *Energy Environ. Sci.*, 5, 5994-6011.

[89] Huang, J.H., Huang, A.T., Hsu, C.Y., Lin, J.T., Chu, C.W. 2012. Influence of molecular weight on silole-containing cyclopentadithiophene polymer and its impact on the electrochromic properties. *Solar Energy Mater. Solar Cells*, 98, 300-307.

[90] Lu, G., Usta, H., Risko, C., Wang, L., Facchetti, A., Ratner, M.A., Marks, T.J. 2008. Synthesis, characterization, and transistor response of semiconducting silole polymers with substantial hole mobility and air stability. *Experiment and theory. J. Am. Chem. Soc.*, 130, 7670-7685.

[91] Usta, H., Lu, G., Facchetti, A., Marks, T.J. 2006. Dithienosilole- and Dibenzosilole-Thiophene Copolymers as Semiconductors for Organic Thin-Film Transistors. *J. Am. Chem. Soc.*, 128, 9034-9035.

- [92] Hou, J., Chen, T.L., Zhang, S., Chen, H.Y., Yang, Y. 2009. Poly[4,4-bis(2-ethylhexyl)cyclopenta[2,1-b;3,4-b']dithiophene-2,6-diyl-alt-2,1,3-benzoselenadiazole-4,7-diyl], a New Low Band Gap Polymer in Polymer Solar Cells. *J. Phys. Chem. C*, 113, 1601-1605.
- [93] Ta-Ya, C., Lu, J., Beaupr, S., Zhang, Y., Pouliot, J.R., Wakim, S., Zhou, J., Leclerc, M., Li, Z., Ding, J., Tao, Y. 2011. Bulk Heterojunction Solar Cells Using Thieno[3,4-c]pyrrole-4,6-dione and Dithieno[3,2-b:2',3'-d]silole Copolymer with a Power Conversion Efficiency of 7.3%. *J. Am. Chem. Soc.*, 133, 4250-4253.
- [94] Zhang, M., Fan, H., Guo, X., He, Y., Zhang, Z., Min, J., Zhang, J., Zhao, G., Zhan, X., Li, Y. 2010. Synthesis and Photovoltaic Properties of Bithiazole-Based Donor-Acceptor Copolymers. *Macromolecules*, 43, 5706-5712.
- [95] Zhu, Z., Waller, D., Gaudiana, R., Morana, M., Muhlbacher, D., Scharber, M., Brabec, C. 2007. Panchromatic Conjugated Polymers Containing Alternating Donor/Acceptor Units for Photovoltaic Applications. *Macromolecules*, 40, 1981-1986.
- [96] Hong, Y.R., Wong, H.K., Moh, L.C.H., Tan, H.S., Chen, Z.K. 2011. Polymer solar cells based on copolymers of dithieno[3,2-b:2',3'-d]silole and thienopyrroledione. *Chem. Commun.*, 47, 4920-4922.
- [97] Huo, L., Chen, H.Y., Hou, J., Chen, T.L., Yang, Y. 2009. Low band gap dithieno[3,2-b:2',3'-d]silole-containing polymers, synthesis, characterization and photovoltaic application. *Chem. Commun.*, 5570-5572.
- [98] Ponomarenko, S.A., Kirchmeyer, S. 2011. Conjugated Organosilicon Materials for Organic Electronics and Photonics. *Adv. Polym. Sci.*, 235, 33-110.
- [99] Somani, P.R., Radhakrishnan, S. 2002. Electrochromic materials and devices: present and future. *Mater. Chem. Phys.*, 77, 117-133.
- [100] Cirpan, A., Argun, A., Grenier, C.R.G., Reeves, B.D., Reynolds, J.R. 2003. Electrochromic devices based on soluble and processable dioxythiophene polymers. *J. Mater. Chem.*, 13, 2422-2428.